UNIVERSITÉ DU QUÉBEC À RIMOUSKI

CONDITIONS OCÉANOGRAPHIQUES DANS LES CANYONS SOUS-MARINS DE POINTE-DES-MONTS

MÉMOIRE PRÉSENTÉ

dans le cadre du programme de maîtrise en océanographie

en vue de l'obtention du grade de maître ès sciences

PAR

©KHOULOUD BACCARA

Août **2023**

Composition du jury :

Cédric Chavanne, président du jury, UQAR-ISMER

Daniel Bourgault, directeur de recherche, UQAR-ISMER

Urs Neumeier, codirecteur de recherche,UQAR-ISMER

Alexandre Normandeau, examinateur externe, Pêches et Océans Canada

Dépôt initial le 28 avril 2023 Dépôt final le 18 août 2023

UNIVERSITÉ DU QUÉBEC À RIMOUSKI

Service de la bibliothèque

Avertissement

La diffusion de ce mémoire ou de cette thèse se fait dans le respect des droits de son auteur, qui a signé le formulaire « *Autorisation de reproduire et de diffuser un rapport, un mémoire ou une thèse* ». En signant ce formulaire, l'auteur concède à l'Université du Québec à Rimouski une licence non exclusive d'utilisation et de publication de la totalité ou d'une partie importante de son travail de recherche pour des fins pédagogiques et non commerciales. Plus précisément, l'auteur autorise l'Université du Québec à Rimouski à reproduire, diffuser, prêter, distribuer ou vendre des copies de son travail de recherche à des fins non commerciales sur quelque support que ce soit, y compris l'Internet. Cette licence et cette autorisation n'entraînent pas une renonciation de la part de l'auteur à ses droits moraux ni à ses droits de propriété intellectuelle. Sauf entente contraire, l'auteur conserve la liberté de diffuser et de commercialiser ou non ce travail dont il possède un exemplaire.

REMERCIEMENTS

Je tiens tout d'abord à exprimer ma profonde gratitude envers mon directeur de recherche, Daniel Bourgault, et mon co-directeur, Urs Neumeier, pour m'avoir offert cette opportunité. Merci infiniment pour votre encadrement bienveillant, et votre confiance. La réussite de ce projet est largement due à votre expertise.

Je tiens également à remercier Cédric Chavanne pour son aide dans l'analyse des données et l'explication des méthodes, ainsi que pour sa disponibilité et son accessibilité.

Je remercie également les membres de jury pour le temps et l'attention qu'ils ont consacrés à l'examen de mon travail.

Je suis profondément reconnaissante envers l'Institut des sciences de la mer de Rimouski (ISMER), le Réseau québéc maritime (RQM) et le Marine Environmental Observation, Prediction and Response Network (MEOPAR) pour leur soutien financier dans la réalisation de ce projet.

Je tiens également à remercier l'équipage du Coriolis II, notamment Christian Boutot et Bruno Cayouette, pour leur travail en mer, la préparation des instruments et la récupération des données. Je remercie également Sylvain Joly pour le traitement des données de vagues.

Je voudrais exprimer ma profonde gratitude envers toutes les personnes qui m'ont accompagné durant ces deux dernières années, malgré les défis rencontrés en raison de la pandémie. Fatma Dhifallah et Safwen Khamassi, vous avez été ma famille à Rimouski. Je vous remercie du fond du cœur d'avoir été constamment à mes côtés, de m'avoir écouté et encouragé. Vous avez été une source de force et de soutien pour moi, et je ne pourrai jamais assez vous remercier. Mes collégue du bureau Maëla Le Ménec, Jonathan Tessirt et surtout Abigaelle Dussol et Rosalie Shink, je suis très reconnaissante de votre soutien, de vos encouragements et de la bonne ambiance au bureau. Vous avez créé un environnement de travail agréable et positif qui a rendu cette expérience encore plus enrichissante. Votre présence a

été d'une grande aide et m'a motivé tout au long de cette aventure. Marwa Khémir, merci beaucoup pour tout ce que tu as fait pour moi. Ta présence, même si c'était à distance, ainsi que tes conseils ont été d'une grande importance pour moi.

Enfin, je souhaite remercier mes parents pour leur amour, leur soutien inconditionnel et leur patience.

RÉSUMÉ

Les canyons sous-marins sont des incisions morphologiques dans les marges continentales agissant comme les conduits préférentiels de sédiments des plateaux continentaux vers l'océan profond. Les mécanismes exacts impliqués dans le transport des sédiments au sein de certains canyons sous-marins, en particulier ceux dont la tête est loin de l'approvisionnement sédimentaire côtier ou fluvial, sont encore mal compris. Pour étudier les processus par lesquels les sédiments sont transportés dans les canyons de Pointe-des-Monts (rive nord de l'estuaire maritime du Saint-Laurent, Canada), deux ADCP (Profileurs de courant Doppler acoustique), un regardant vers le haut et l'autre vers le bas ont été déployés à 155 mètres de profondeur entre octobre 2020 et octobre 2021. Vingt-cinq heures de profils de salinité et de température en octobre 2020 et en octobre 2021 ont fourni une vue d'ensemble des conditions océanographiques et des cycles tidaux. L'analyse des vitesses horizontales et verticales près du fond et l'intensité des échos de retour de l'ADCP ont permis d'identifier deux processus principaux de transport de sédiments opérant le long de ce canyon. Le premier est les mascarets internes, causés par la marée interne semi-diurne, générés le long du canyon. Ce processus pourrait remettre en suspension de fines particules et les transporter vers la tête du canyon avec la propagation de l'onde de marée interne. Une occurrence régulière de ces mascarets internes a été enregistrée (532 mascarets internes identifiés pour 362 jours). Leur occurrence la plus élevée est à l'heure de la marée interne basse, quelle que soit la saison et la phase de la marée de surface. Le deuxième est associé aux courants de turbidité, qui avaient déjà été documentés dans les canyons de Pointe-des-Monts dans des études précédentes. Au cours de la période 2020-2021, un seul courant de turbidité s'est produit, caractérisé par une augmentation soudaine de la vitesse vers l'aval du canyon et des valeurs élevées d'échos de retour de l'ADCP. Cette turbidite est beaucoup plus énergétique que les mascarets et elle a possiblement transporté de grands volumes de sédiments vers l'aval. Elle a été déclenchée pendant une tempête.

Mots clés : Canyon sous-marin, Transport de sédiments, Marée interne, Courants de turbidité, Mascaret interne.

ABSTRACT

Submarine canyons are morphological incisions in continental margins, acting as the preferential conduits of sediments from the continental shelves to the deep ocean. The exact mechanisms involved in the transport of sediments within certain submarine canyons are still poorly understood, in particular when the canyon head is far from the coastal or fluvial sedimentary supply. To study the processes by which sediments are transported in the canyons of Pointe-des-Monts (north shore of the lower St. Lawrence estuary, Canada), two ADCP (Acoustic Doppler current profiler), one looking up and the other down were deployed at 155 meters depth from October 2020 until October 2021. Twenty-five hours of salinity and temperature profiles in October 2020 and in October 2021 provided an overview of oceanographic conditions and tidal cycles. Analysis of near-bottom horizontal and vertical velocities and intensity of ADCP backscatter identified two main sediment transport processes operating along this canyon. The first is the internal tidal bores, caused by the semi-diurnal internal tide, generated along the canyon. This process may resuspend fine particles and transport them to the head of the canyon with the propagation of the internal tidal wave. A regular occurrence of these internal bores was recorded (532 internal bores identified for 362 days). Their highest occurrence is at the time of low internal tide, regardless of the season and the phase of the surface tide. The second is turbidity currents, which have already been documented in the Pointe-des-Monts canyons in previous studies. During the 2020-2021 period, a single turbidity current occurred, characterized by a sudden increase of down-canyon velocity and high values of ADCP backscatter. This turbidite is much more energetic than the tidal bores and likely transported large volumes of sediment downstream. It was presumably triggered during a storm.

Keywords : Submarine canyon, Sediment transport, Internal tide, Turbidity currents, Internal tidal bore.

TABLE DES MATIÈRES

LISTE DES TABLEAUX

LISTE DES FIGURES

INTRODUCTION GÉNÉRALE

Les canyons sous-marins sont des vallées abruptes incisées dans le talus continental formés par des écoulements de sédiments. Ce sont par ailleurs les principaux conduits par lesquels les sédiments continentaux sont transportés vers le fond marin. Dans certains cas, les canyons incisent le plateau continental jusqu'à une profondeur de l'ordre de 100 m et transfèrent les sédiments côtiers à des profondeurs de plus de 1000 m, principalement par des écoulements gravitaires (Normandeau et al., 2015). Les sédiments qui traversent les canyons sous-marins proviennent principalement des rivières, des calottes glaciaires, de la dérive littoral ou la remobilisation des sédiments du plateau (Normandeau et al., 2014).

Un canyon sous-marin est défini comme actif lorsqu'il y a une remise en suspension et un transport fréquent des sédiments du plateau vers le fonds marin. L'activité des canyons sous-marins dépend largement du taux d'apport de sédiments à leur tête et des processus océanographiques capables de remobiliser ces sédiments (Puig et al., 2014). À l'échelle de temps géologique, le concept de stratigraphie séquentielle met l'accent sur les variations du niveau marin relatif en tant que contrôle majeur du transport des sédiments dans les canyons sous-marins. L'augmentation et la diminution de l'apport de sédiments fluviaux à la tête des canyons sont associées respectivement à l'abaissement et l'élévation du niveau de la mer. Lorsque le niveau de la mer monte, la majeure partie du plateau est submergée et les distances entre l'embouchure de la rivière et la tête du canyon augmentent, entrainant une réduction de l'apport de sédiments fluviaux. Par conséquent, l'érosion des canyons avec les flux de sédiments générés par les apports fluviaux diminue et les canyons deviennent inactifs (Chiang and Yu, 2022). Cependant, Paull et al. (2002), Boyd et al. (2008) et Babonneau et al. (2013) ont démontré que l'activité des canyons ne dépend pas nécessairement des positions du niveau marin relatif, comme le suggéraient précédemment les modèles de stratigraphique séquentielle. De nombreux canyons sous-marins du monde sont actuellement actifs malgré le haut niveau marin actuel, qui est censé diminuer ou stopper leur activité.

Leur activité est plutôt contrôlée par leur proximité à une source de sédiments, car l'activité des canyons dépend largement du taux d'apport de sédiments à leur tête et des conditions océanographiques et climatiques. Par conséquent, les canyons sont généralement considérés comme inactifs lorsqu'aucun sédiment n'est disponible à proximité de leur tête (Normandeau et al., 2014). Les facteurs tectoniques et climatiques, ainsi que le type et le volume des sédiments, jouent aussi un rôle majeur dans l'activité des canyons. Par exemple, les processus tectoniques influencent la largeur et la pente du plateau continental et la sensibilité du continent à l'érosion et ils sont connus pour avoir un rôle important dans l'activité des canyons. Le type et le volume de sédiments incluent la capacité d'un matériau à être érodé et transporté, tandis que le climat influence largement les précipitations, qui à leur tour influencent les crues des rivières et l'apport de sédiments à la côte. Tous ces processus peuvent avoir plus d'impact que les positions du niveau marin relatif sur l'activité du canyon (Normandeau et al., 2015).

Boyd et al. (2008) et Ducassou et al. (2009) ont montré que malgré l'éloignement de l'embouchure de la rivière de la tête du canyon et le niveau marin actuel l'activité dans les canyons peut être soutenue par les tempêtes qui peuvent engendrer la remobilisation des sédiments côtiers et leur transfert sous forme de courants de turbidité. Ces courants de turbidité sont générés à la tête canyons et non pas sur les plateaux et remobilisent des sédiments précédemment déposés dans les canyons. Ces événements trés énergétiques constituent le principal mécanisme agissant sur la mobilisation des sédiments dans ces canyons (Chiang and Yu, 2022). Les courants de turbidité, encore appelés avalanches de sédiments sous-marins, sont des écoulements de courant de densité entraînés vers le bas par la densité excessif des sédiments en suspension. Ils font partie des processus de transport de sédiments les plus importants. Seuls les systèmes fluviaux terrestres transportent des volumes similaires de sédiments. Les courants de turbidité jouent un rôle important dans le cycle et la séquestration du carbone à l'échelle mondiale et fournissent des nutriments importants aux écosystèmes des grands fonds marins. Leurs dépôts (appelés turbidites) hébergent les principaux réservoirs de pétrole dans le monde et constituent d'importantes archives du passé géologique de la Terre (Azpiroz-Zabala et al., 2017). En revanche, ils représentent des risques majeurs puisqu'ils

peuvent rompre les câbles de communication sous-marins, qui transportent plus de 95 % des données mondiales, les pipelines sous-marins, et les infrastructures pétrolières et gazières (Normandeau et al., 2020).

Contrairement à plusieurs observations directes de la vitesse et de la concentration de sédiments en suspension dans les rivières, il existe peu de mesures directes des courants de turbidité dans les canyons puisque ces flux sous-marins sont difficiles à surveiller en raison de leur emplacement difficile d'accès, de leur occurrence imprévisible et de leur capacité à endommager les instruments placés sur leur chemin. De ce fait, la dynamique fondamentale des courants de turbidité n'est pas suffisamment bien comprise pour permettre de prédire et d'atténuer les risques considérables qu'ils représentent pour les infrastructures sous-marines coûteuses (Azpiroz-Zabala et al., 2017).

Une deuxième question clé sur les courants de turbidité est de savoir comment ils sont déclenchés. Des études antérieures ont pour la plupart déduit que les courants de turbidité ont besoin d'un déclencheur externe majeur, tel qu'un tremblement de terre, une tempête, une crue, ou une combinaison de marée basse et d'un débit fluvial élevé. Cette inférence est importante car elle constitue la base de la prédiction du moment où les courants de turbidité se produisent et de leurs intervalles de récurrence, ce qui est important pour les évaluations des dangers (Paull et al., 2018).

Les mascarets internes sont un autre mécanisme qui peut se produire dans les canyons et qui est susceptible d'occasionner une remise en suspension et un transport de sédiments. Un mascaret est un saut hydraulique qui se produit lorsqu'une marée montante d'amplitude importante pénètre dans des rivières peu profondes, à pente douce et rétrécissant en largeur. Cela provoque une élévation soudaine de la surface d'eau formant une onde solitaire ou une série d'ondes qui se propagent vers l'amont et contre la direction du courant de la rivière. Ils ont un impact important sur le comportement de l'écosystème fluvial, notamment en termes de transport des sédiments (Bonneton et al., 2011). Ce phénoméne peut se produire à chaque cycle de marée (deux fois par jour avec des marées semi-diurnes).

Les mascarets sont caractérisés et classés par le nombre de Froude (Fr) qui est un nombre sans dimension exprimant le rapport des forces inertielles et des forces gravitationnelles. Il est défini comme

$$\mathrm{Fr} = \frac{U}{\sqrt{gh}}, \tag{1}$$

où, g, U et h sont, respectivement, l'accélération de la gravité (m/s^2), la vélocité (m/s), et la profondeur d'écoulement (m). Pour caractériser les mascarets, U est considéré la comme la vitesse du courant de la rivière et de la vitesse du mascaret.

Dans la plupart des cas, le nombre de Froude indique l'intensité et la forme du mascaret, selon les 4 cas suivants :

Fr < 1 : pas de mascaret,

1 < Fr < 1,43 correspond à des mascarets onduleux,

1,43 < Fr < 1,57 correspond à des mascarets partiellement cassants et

Fr > 1,57 correspond à des mascarets totalement cassants (Putra et al., 2021).

Le mascaret interne est analogue au mascaret de surface, mais se produit en profondeur entre deux couches d'eau dans les milieux stratifiés tels que les estuaires et les mers cotières. On peut retrouver des mascarets internes dans les canyons par l'effet des marées internes (ou appelées marées baroclines). Ces marées internes sont des ondes internes de fréquence de marée qui résultent de l'interaction de la marée barotrope avec une topographie variable telle qu'au niveau des canyons sous-marins et dans une colonne d'eau stratifiée. En se propageant, ces marées internes entrainent la formation d'ondes internes non linéaires qui sont les mascarets internes (Pritchard and Weller, 2005). Commes les marées internes se produisent à l'interface de deux masses d'eau avec des densités différentes, ces mascarets internes donnent lieu à un changement brusque de température et de densité. Comme les vagues de surface, les mascarets internes peuvent déferler, ce qui entraîne un mélange turbulent des masses d'eaux. Ce processus influence la remise en suspension des sédiments du fond. Les mascarets internes

sont également caractérisés par le nombre de Froude interne définie par

$$\mathrm{Fr}_i = \frac{U'}{\sqrt{g'h}}, \tag{2}$$

où U' est la vélocité de la couche interne (m/s), h son épaisseur (m), g' est la gravité réduite (m/s^2) définie par : g'=g($\Delta\rho/\rho_0$) et $\Delta\rho$ est la différence de densité entre les deux couches (Holloway, 1987).

Pour le cas des mascarets internes Masunaga et al. (2019) indiquent que le nombre de Froude interne peut s'exprimer par

$$\mathrm{Fr}_i = \frac{a}{\lambda}, \tag{3}$$

où a est l'amplitude de l'onde interne et λ est la longeur d'onde. L'intensité de la turbulance due au déferlement des mascarets internes dépend du rapport de la pente topographique et de la racine de Fr_i défini comme le nombre d'Iribarren interne (ζ)

$$\zeta = \frac{s}{\sqrt{\mathrm{Fr}_i}}, \tag{4}$$

où s est la pente.

Les mascarets internes sont classés en deux catégories générales en fonction du nombre d'Iribarren interne, chacun avec une dynamique distincte et des qualités de mélange turbulent. La première catégorie sont les mascarets internes canoniques qui se produisent pour une pente douce ou une vague abrupte ($\zeta << 1$) où l'intensité de la turbulence due au déferlement est forte et, par conséquent, presque toute l'énergie des ondes internes entrante est perdue en raison du mélange turbulent et de la dissipation lors de la rupture. Dans cette situation, les ondes internes s'élèvent progressivement sur une faible pente créant un front de vague raide accompagné d'une forte baisse de température au cours du temps, suivie d'un front d'onde variant graduellement accompagné d'une lente augmentation de la température avec le temps (Fig. 1c). Une fois que la marée interne qui a généré le mascaret interne commence à se

retirer, ce dernier continue de se propager vers le haut comme un noyau de vortex qui finit par se dissiper dans les eaux moins profondes (Fig. 1a).

La deuxième catégorie sont les mascarets internes non canoniques, se produisant sur une topographie abrupte ou une faible pente d'onde ($\zeta \approx 1$) où l'intensité de la turbulence est faible et la plupart de l'énergie des vagues entrantes se reflète au large. Le signal de température associé à ces mascarets internes montre une diminution progressive de température au passage du mascaret, suivie d'une augmentation rapide de la température lorsque le mascaret interne recule (Fig. 1bd) (Masunaga et al., 2019).

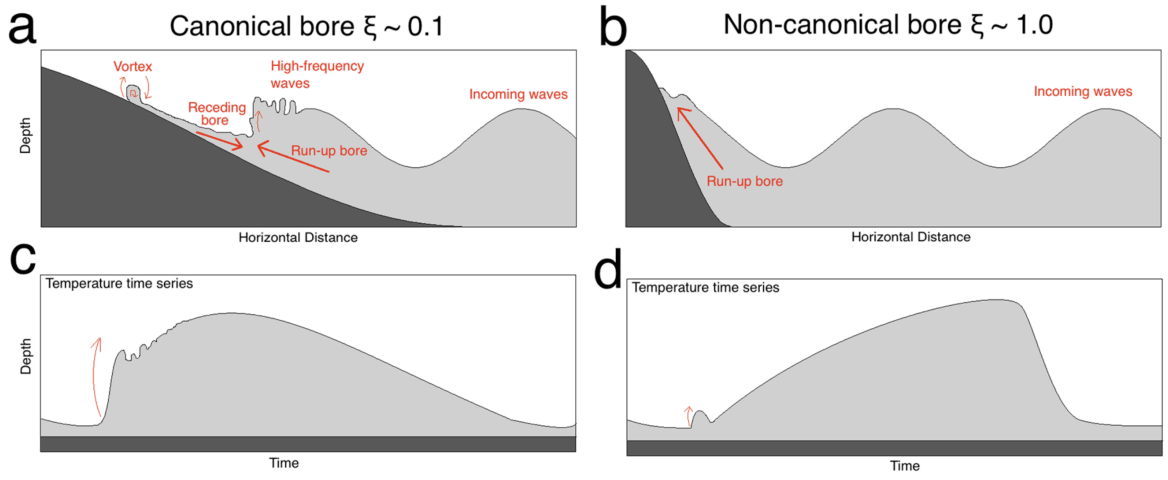

FIGURE 1: Schémas des mascarets canoniques (a, c) et des mascarets non canoniques (b, d). Panneaux supérieurs (a, b) montrent la coupe verticale de la structure de vague et les panneaux inférieurs (c, d) montrent la série temporelle température/densité sur une pente. La couleur gris clair indique une eau plus dense ou plus froide (Masunaga et al., 2019).

Bien que l'importance des ondes internes pour le transport et le mélange dans l'océan est connu, les détails des processus de déferlement et de mélange des mascarets internes restent mal compris en raison de la difficulté de mesurer ce phénomène (Masunaga et al., 2016). Des mascarets internes ont été observés dans un certain nombre de canyons notamment dans la baie de Californie du Sud (Pineda, 1994), dans de nombreux endroits sur le plateau

continental nord de la Californie (Howell and Brown, 1985), et sur la côte nord-ouest en Australie (Lauton et al., 2021). Il a été démontré que ces mascarets internes induisent un transport important de sédiments et des turbulences près des têtes de canyon. Pineda (1994) a documenté que les mascarets internes produisaient une remontée d'eau qui pourrait ainsi induire une mobilisation des sédiments.

Des études plus récentes (Hill et al., 2008; Conway et al., 2012; Clarke et al., 2014) sur des canyons sous-marins peu profonds à l'aide d'échosondeurs multifaisceaux à haute résolution ont permis de cartographier à haute résolution et de réaliser des images en détail des processus sédimentaires récents et fréquents agissant en leur sein. De tels canyons ou chenaux sous-marins peu profonds sont souvent observés à la tête des fjords ou à l'embouchure des rivières. Plus récemment, des canyons sous-marins ont également été découverts dans des secteurs très peu profonds des plateaux continentaux à des profondeurs inférieures à 60 m ainsi plus d'attention est maintenant donnée à ces systèmes à petite échelle dans des environnements peu profonds du fait qu'ils peuvent être cartographiés à haute résolution et peuvent fournir une bonne visualisation des processus hydrodynamiques (Normandeau et al., 2015).

Des systèmes similaires en eaux peu profondes ont été signalés dans l'estuaire du Saint-Laurent, en particulier dans les canyons sous-marins de Pointe-des-Monts (Normandeau et al., 2015). Ces canyons sont situés dans l'estuaire maritime du Saint-Laurent, à l'extrémité ouest du golfe du Saint-Laurent (Fig. 2). Ils ont une longueur de moins de 3.5 km à plus de 300 m de profondeur. Leur largeur varie entre 100 et 300 m. Les deux plus grandes rivières de la région sont la rivière Baie-Trinité et la rivière Godbout, situées à 12 km à l'est et à l'ouest des canyons. Des ruisseaux sont aussi observés entre Baie-Trinité et Pointe-des-Monts, mais ils ne sont pas directement à la tête des canyons (Normandeau et al., 2014). Des mesures répétées de bathymétrie multifaisceaux, Normandeau et al. (2014) ont démontrés grâce à l'observation de formes en croissant, que les canyons de Pointe-des-Monts sont en réalité actifs malgré qu'il y ait très peu de sédiments à leur tête. Ces formes en

croissant sont liées aux passages répétés de courants de turbidité (Normandeau et al., 2020). Aussi, les variations bathymétriques dues au déplacements des formes en croissant entre les deux campagnes bathymétriques de 2007 et 2012 ont dépassé 2,5 m (Normandeau et al., 2014). De plus, des courants de turbidité ont été identifiés dans les dépôts sédimentaires dans la zone profonde devant les canyons (Normandeau, 2015), et d'autres ont été enregistrés par des ADCP (courantomètres acoustiques à effet doppler) (Normandeau et al., 2020).

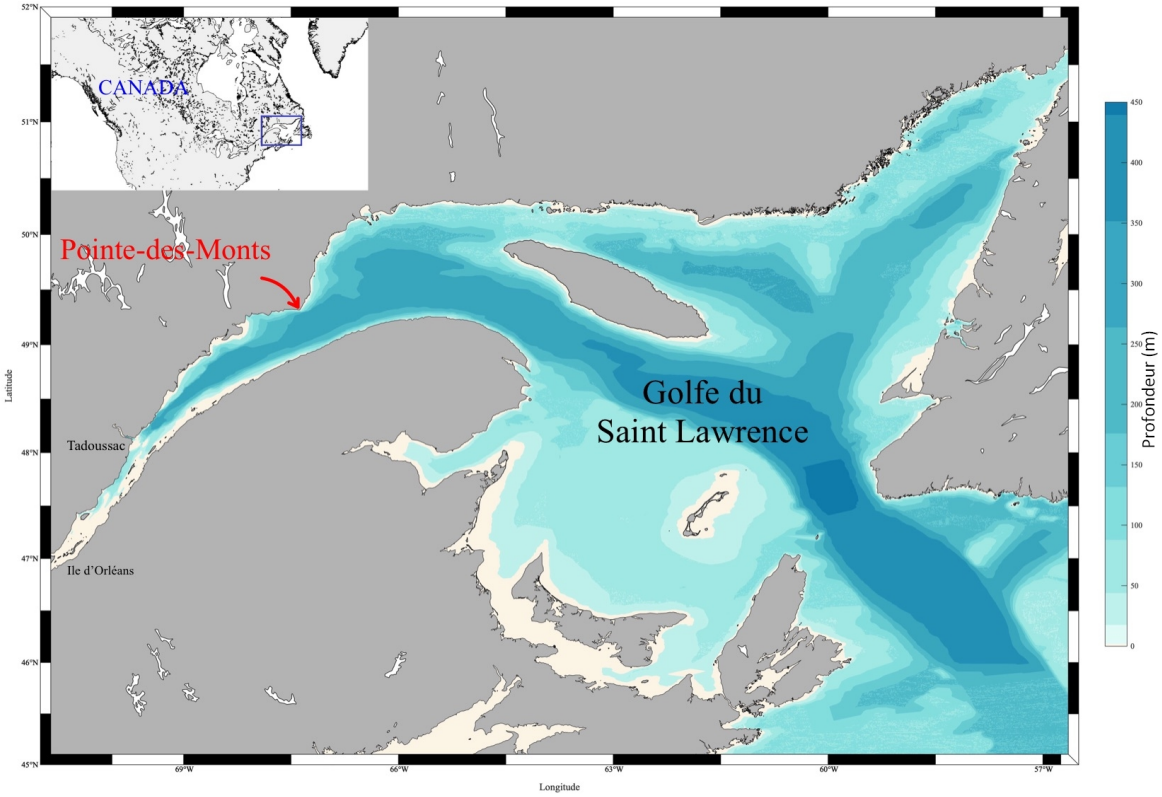

FIGURE 2: Localisation des canyons de Pointe-des-Monts

Les canyons sous-marins de Pointe-des-Monts sont les seuls dans l'estuaire maritime du Saint-Laurent classés parmi les canyons pauvres en sédiments (Normandeau et al., 2014). Ce sont également les seuls canyons montrant des signes d'activités fréquentes, bien que l'apport de sédiments soit minimes à leur tête, alors que d'autres secteurs de l'estuaire maritime (par exemple : les Escoumins) ont des paramètres physiques similaires et un apport

sédimentaire plus important, mais ne présentent que peu ou pas de signes d'activité récente d'écoulement gravitaire. Cependant, comme les canyons de Pointe-des-Monts sont situés sur une pente raide, les instabilités de pente et les processus hydrodynamiques peuvent remobiliser leurs sédiments, entraînant des écoulements gravitaires actifs. Ceci confirme que l'apport de sédiments n'est pas nécessairement un contributeur important aux processus d'écoulement gravitaire dans les estuaires et les environnements de l'intérieur du plateau (Normandeau et al., 2015).

Problématique et objectif :

Ce projet de maitrise fait partie d'un programme de recherche multidisciplinaire plus large dont la problématique générale est d'étudier les processus hydrodynamiques et les risques naturels engendrés par la remobilisation des sédiments et leurs impacts sur la dynamique de la productivite primaire dans l'estuaire du Saint-Laurent. La remise en suspension des sédiments induite par les courants de turbidité a déjà été documentée à Pointe-des-Monts lors de tempêtes, mais la compréhension complète de ses causes (tempêtes, marées internes, etc.) nécessite des investigations plus approfondies. De même, il a déjà été démontré dans d'autres systèmes côtiers que les mascarets internes peuvent induire un important transport sédimentaire et beaucoup de turbulence. À Pointe-des-Monts, des mesures de courantomètres à effet Doppler (ADCP) suggèrent l'existence de mascarets internes, mais les observations sont encore insuffisantes pour confirmer leur présence et comprendre leur fonctionnement dynamique. Les données nécessitent d'être analysées plus en profondeur.

L'objectif de ce projet est de décrire et présenter les conditions océanographiques dans les canyons sous-marins de Pointe-des-Monts et particulièrement d'identifier les processus hydrodynamiques qui contribuent à la mobilisation et remise en suspension des sédiments le long de l'axe du canyon. Plus spécifiquement, nous allons :

1. Identifier, comptabiliser et caractériser les courants de turbidité à Pointe-des-Monts entre 2020 et 2021 dans le but de déterminer leurs causes.

2. Identifier, comptabiliser et caractériser les mascarets internes afin de distinguer leur rôle dans la dynamique sédimentaire des canyons.

CHAPITRE I

OCEANOGRAPHIC CONDITIONS IN THE SUBMARINE CANYONS OF POINTE-DES-MONTS

1.1 Résumé en français de l'article

Les canyons sous-marins sont des incisions morphologiques dans les marges continentales agissant comme les conduits préférentiels de sédiments des plateaux continentaux vers l'océan profond. Les mécanismes exacts impliqués dans le transport des sédiments au sein de certains canyons sous-marins, en particulier ceux dont la tête est loin de l'approvisionnement sédimentaire côtier ou fluvial, sont encore mal compris. Pour étudier les processus par lesquels les sédiments sont transportés dans les canyons de Pointe-des-Monts (rive nord de l'estuaire maritime du Saint-Laurent, Canada), deux ADCP (Profileurs de courant Doppler acoustique), un regardant vers le haut et l'autre vers le bas ont été déployés à 155 mètres de profondeur entre octobre 2020 et octobre 2021. Vingt-cinq heures de profils de salinité et de température en octobre 2020 et en octobre 2021 ont fourni une vue d'ensemble des conditions océanographiques et des cycles tidaux. L'analyse des vitesses horizontales et verticales près du fond et l'intensité des échos de retour de l'ADCP ont permis d'identifier deux processus principaux de transport de sédiments opérant le long de ce canyon. Le premier est les mascarets internes, causés par la marée interne semi-diurne, générés le long du canyon. Ce processus pourrait remettre en suspension de fines particules et les transporter vers la tête du canyon avec la propagation de l'onde de marée interne. Une occurrence régulière de ces mascarets internes a été enregistrée (532 mascarets internes identifiés pour 362 jours). Leur occurrence la plus élevée est à l'heure de la marée interne basse, quelle que soit la saison et la phase de la marée de surface. Le deuxième est associé aux courants de turbidité, qui avaient déjà été documentés dans les canyons de Pointe-des-Monts dans des études précédentes. Au

cours de la période 2020-2021, un seul courant de turbidité s'est produit, caractérisé par une augmentation soudaine de la vitesse vers l'aval du canyon et des valeurs élevées d'échos de retour de l'ADCP. Cette turbidite est beaucoup plus énergétique que les mascarets et elle a possiblement transporté de grands volumes de sédiments vers l'aval. Elle a été déclenchée pendant une tempête.

1.2 Abstract

Submarine canyons are morphological incisions on continental margins, acting as the preferential conduits of sediments from the continental shelves to the deep ocean. The exact mechanisms involved in the transport of sediments within certain submarine canyons are still poorly understood, in particular when the canyon head is far from the coastal or fluvial sedimentary supply. To study the processes by which sediments are transported in the canyons of Pointe-des-Monts (north shore of the lower St. Lawrence estuary, Canada), two ADCP (Acoustic Doppler current profiler), one looking up and the other down were deployed at 155 meters depth from October 2020 until October 2021. Twenty-five hours of salinity and temperature profiles in October 2020 and in October 2021 provided an overview of oceanographic conditions and tidal cycles. Analysis of near-bottom horizontal and vertical velocities and intensity of ADCP backscatter identified two main sediment transport processes operating along this canyon. The first is the internal tidal bores, caused by the semi-diurnal internal tide, generated along the canyon. This process may resuspend fine particles and transport them to the head of the canyon with the propagation of the internal tidal wave. A regular occurrence of these internal bores was recorded (532 internal bores identified for 362 days). Their highest occurrence is at the time of low internal tide, regardless of the season and the phase of the surface tide. The second is turbidity currents, which have already been documented in the Pointe-des-Monts canyons in previous studies. During the 2020-2021 period, a single turbidity current occurred, characterized by a sudden increase of down-canyon velocity and high values of ADCP backscatter. This turbidite is much more energetic than the

tidal bores and likely transported large volumes of sediment downstream. It was presumably triggered during a storm.

1.3 Introduction

Submarine canyons are morphological features found on many continental margins and serve as preferential conduits for transporting sediments from the continental shelf to deep-sea environments. Sediment-gravity mechanisms (i.e., turbidity currents, debris flows) dominate the transport volume through submarine canyons, carrying large volumes of terrestrial sediments to deeper parts of the continental margin (Puig et al., 2013). Although the Holocene sea level rise has reduced drastically the supply of sediments to submarine canyons, many contemporary submarine canyons are still active, exporting significant amount of sediments from the shelf to greater depths. Some canyons remain active due to their proximity or direct connection to fluvial systems. However, proximity to river mouths is not a requirement for canyon activity. In canyons that are far from river mouths and disconnected from river input, sediments are carried down to the deep ocean by the action of storms, earthquakes, spontaneous destabilization of sediments, and even human activity (Martín et al., 2011). Recent in-situ measurements in those kinds of canyons showed important sediment fluxes, most of them related to storm-related turbidity currents (Martín et al., 2011).

Turbidity currents largely dominate the present-day transfer of sediment through canyons. However, they are not the only active process in deep sediment transport mechanisms. Internal tidal bottom currents dominate the flow in many submarine canyons (Xu et al., 2008). They generate internal tidal bores, which is a type of internal surge propagating upstream that occurs within a stratified fluid. Internal tidal bores are generated when a rising internal tide with significant amplitude enters shallow, gently sloping, and narrowing areas which causes the displacement of the stratified layers of water. As the wave travels along, it can cause strong currents, turbulence, and mixing of the water column (Bonneton et al., 2011).

They are recognized as efficient forcing for sediment transport and resuspension, as they can reach maximum velocities of 25-50 cm/s (Shanmugam, 2003). Internal tides can be generated under favorable conditions of topography and vertical stratification, which can significantly enhance energy flux in canyons compared with the barotropic tide (Mulder et al., 2012). In-situ measurements in canyons located in southern California demonstrated the impact of internal tidal bores in sediment resuspension (Pineda, 1994). A similar phenomenon is also suspected to be occurring in the Pointe-des-Monts canyons. However, there is no evidence that such processes explain permanent sediment-transport observations.

In Pointe-des-Monts canyons, such hydrodynamic patterns are still poorly documented and there is scarce evidence of their effect on sedimentary processes. During the last few years, the Pointe-des-Monts canyons have been the subject of several field studies (Normandeau et al., 2014, 2015, 2020, 2022), most of them have collected current and backscatter data of moored current profilers (ADCP) and high-resolution multibeam bathymetry. The motivation of these studies was to collect field data to understand the processes that trigger turbidity currents. These studies have provided information about contemporary sediment-transport processes acting within submarine canyons by means of analysis of combined climate, currents, and suspended-sediment concentration data. They suggest that a large external trigger such as storms is required to initiate turbidity currents in sediment-starved environments and a complete understanding of turbidity current triggers and canyon morphodynamics is necessary for risk reduction (Normandeau et al., 2020).

This paper presents a detailed description of the oceanographic conditions of the Pointe-des-Monts canyons between 2020 and 2021. It focuses on storm-induced turbidity currents and internal bores that contribute to sediment transport processes along the canyon axis by analyzing ADCP mooring data (bottom water velocity and backscatter intensities).

1.4 Regional background

The St. Lawrence Estuary is one of the largest estuaries in the world (8000 km^2), glacially carved during past glaciations, reaching 200 km in length, 50 km in width and ≤350 m in depth (Normandeau et al., 2015). It is located in Quebec (eastern Canada) in a temperate-subarctic climate with 2-4 months of sea-ice in winter (Fig. 2). The St. Lawrence Estuary is divided into two parts based on the characteristics of the bottom topography. The Upper estuary, extending from Ile d'Orleans to Tadoussac, is narrow (2 to 24 km wide) with depths averaging to 60 m and several sills. In contrast, the Lower St. Lawrence Estuary, which stretches from Tadoussac to Pointe-des-Monts, where the Gulf of St begins. Lawrence Estuary is characterized by the Laurentian Trough, a wide and deep submarine valley extending from Tadoussac through the Gulf of St. Lawrence to the edge of the continental shelf south of Newfoundland. The slopes of the Laurentian Trough are mostly shaped by mass-transport deposits and a series of submarine canyons (Mertz and Gratton, 1990). The origin of these canyons is still uncertain, although Pinet et al. (2011) indicated that they are Holocene in age.

The Lower St. Lawrence Estuary is characterized by large spatiotemporal variations of the water stratification with the presence of a cold intermediate layer (CIL) during summer and fall being its distinctive feature. This layer is mostly formed in situ in the Gulf of St. Lawrence during the previous winter by atmospheric cooling (Koutitonsky and Budgen, 1991; Galbraith, 2006). Over the rest of the year, the water column is characterized by a two-layer system. The winter surface layer occupies the upper ~ 75 m (salinity >= 32 PSU and temperature about -1.7 °C), and the deep layer is located below (temperature between 1 and 7 °C and salinity between 32 and 35 PSU (Bourgault et al., 2017).

In the Pointe-des-Monts sector, three distinct and well-developed submarine canyons that incise quaternary sediments along the slope offshore are observed (Fig. 3) (Normandeau et al., 2015). The Pointe-des-Monts coastline is stable, without signs of active erosion. The coast is almost entirely rocky and overlain only by very thin and isolated sediment patches.

The shoreline and shelf are composed of metasedimentary gneisses and crystalline limestone. Within a 5 km range on both sides of the canyons, 16% of the shoreline is covered by sand beaches. Between 2007 and 2012 no major sedimentation occurred at the head of the canyons (Normandeau et al., 2014).

This study looks at the conditions in the eastern canyons (canyon "C3" on Fig. 3), which has similar physical settings as the canyon "C2". Canyon "C3" starts at 300 m from the shore and has a length of 4.5 km, from the head to the edge of the fans. Its width varies from 100 to 300 m. Its slope can be divided into three sections: (1) Near the head, where the seafloor consists of bedrock, the slope is steep (20°) down to 75 m water depth. (2) Between 75 and 125 m water depth, a thin layer of sediment lies above the bedrock, and the slope decreases to 15°. This section consists of many small gullies that are connected to the main tributaries of the canyons. Gullies exhibit a smooth slope (e.g., lack of escarpment) and are separated by thin (less than 50 m wide) sedimentary ridges that produce 'washed-out' surfaces. (3) The slope of the canyon floor then decreases to 2-3°, from 125 m to 300 m water depth. The relief of the canyon (height margins–thalweg) varies between 10 and 40 m. The analysis of sediment samples collected from C3 fans reveals that the facies in this area is predominantly made up of very fine sand, with an average grain size of approximately 90 micrometers. Small escarpments (less than 100 m in size) are observed along canyon walls. Numerous crescentic bedforms can be seen within the thalweg of the canyons. They are asymmetric downslope, have wavelengths below 60 m, and are 1–3 m high (Normandeau, 2015). The absence of any significant sediment source near the canyon head indicates that these submarine canyons are currently remobilizing sediments already present within them or originating from the erosion of the canyons themselves (Normandeau et al., 2014).

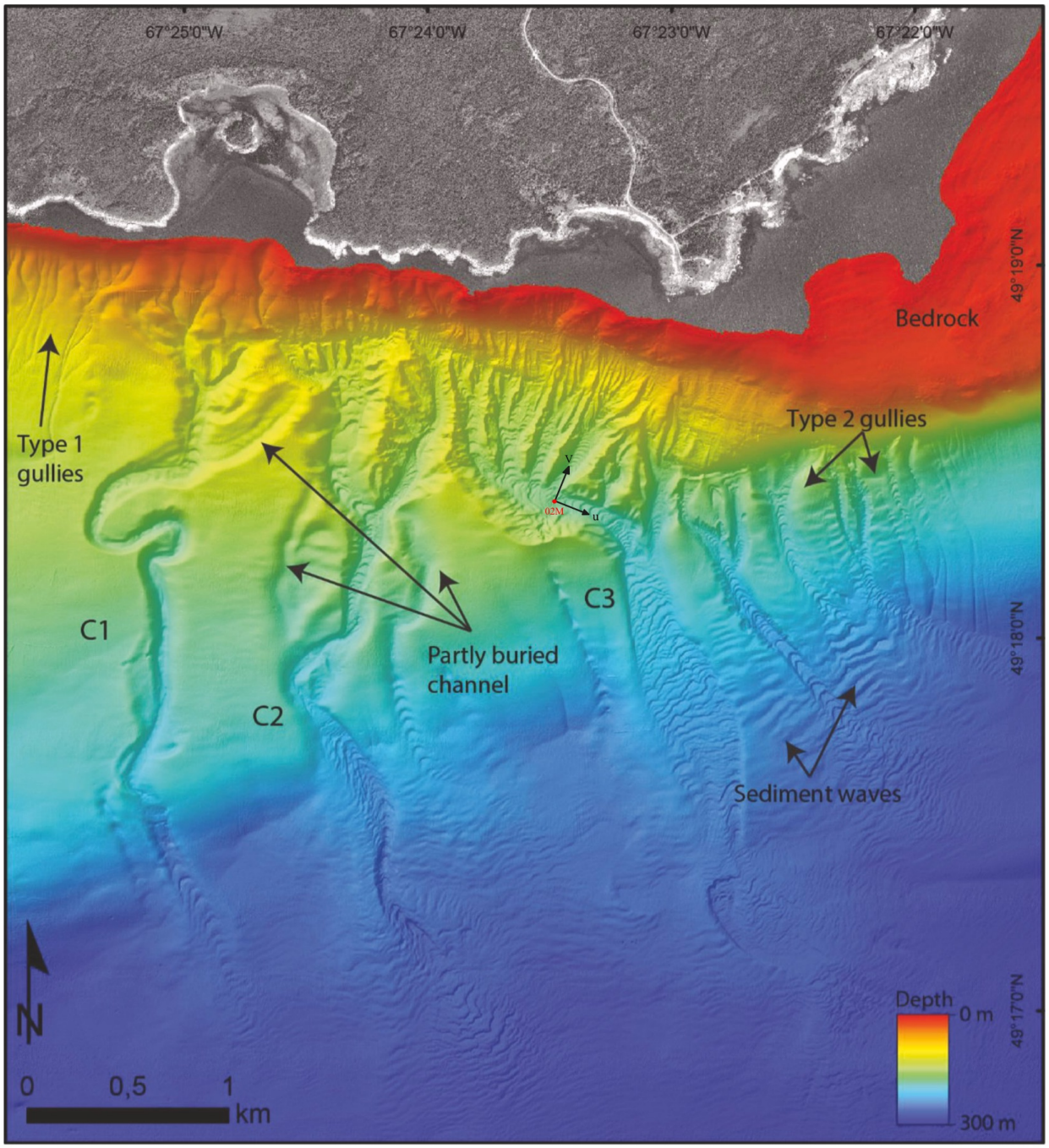

Figure 3: Multibeam bathymetry of the Pointe-des-Monts canyons (Normandeau, 2015). The present study examines the conditions in the canyon ”C3”.The position of the mooring is shown with a small red dot.

1.5 Datasets and Methodology

1.5.1 Mooring

The activity of the Pointe-des-Monts submarine canyons was assessed with a mooring deployed from the R/V Coriolis II at 49°18.398' N/67°23.520' W (Fig. 4) in a water depth of 183 m for 12 consecutive months from 14th October 2020 until 11 October 2021. This mooring is composed of 2 Acoustic Doopler Current Profilers (ADCP), the first mounted 27.5 m above the bottom (mab) and looking downward, the second mounted 28.5 mab and looking upward. The ADCPs recorded velocity profiles, acoustic backscatter profiles, and pressure. Acoustic backscatter intensity, which is a function of sediment concentration and grain size, can be used as proxy for sediment concentration. The downward-looking ADCP was a Teledyne RDI Workhorse 600 kHz sampling one ping every 20 s with a vertical bin size of 1 meter. The upward-looking ADCP was a Teledyne RDI Workhorse 300 kHz sampling one ping every 40 s with a vertical bin size of 4 m. Both ADCPs recorded individual pings. The acoustic beams of both ADCPs are 20° angle respective to a vertical line. The mooring was deployed in the most active canyon C3 and was positioned to capture turbidity currents coming down from any of the upstream gullies. Water temperature and pressure were recorded simultaneously on the same mooring with 2 RBR duet T.D temperature-pressure sensors, the first at 27.5 mab and the second at 5 mab.

Both ADCPs were set up to record in beam coordinates. Data were converted to instrument-coordinates (XYZ) and then to Earth-coordinates (ENU) during post-processing. The ADCPs recorded only small roll and tilt variations during the entire mooring deployment, neither of which went beyond 2.5° and 2.0° from the vertical. Prior to analysis, a quality control was performed on the velocity data. It consists of removing data that fall below the seafloor, are affected by the seafloor due to side lobe interference, have bad values or a too low signal to noise ratio using a graphic interface programmed in Matlab by Urs Neumeier, which allows a visual inspection of the data. upper part of the velocity profiles of

the uplooking ADCP had a bad data quality, this part of the velocity profiles is not shown in this paper.The Tidal analysis of the ADCP and RBR data was performed using the MATLAB Unified Tidal Analysis and Prediction package UTide (Codiga, 2011), and the power spectra were calculated considering the 95 % confidence limit and hamming window.

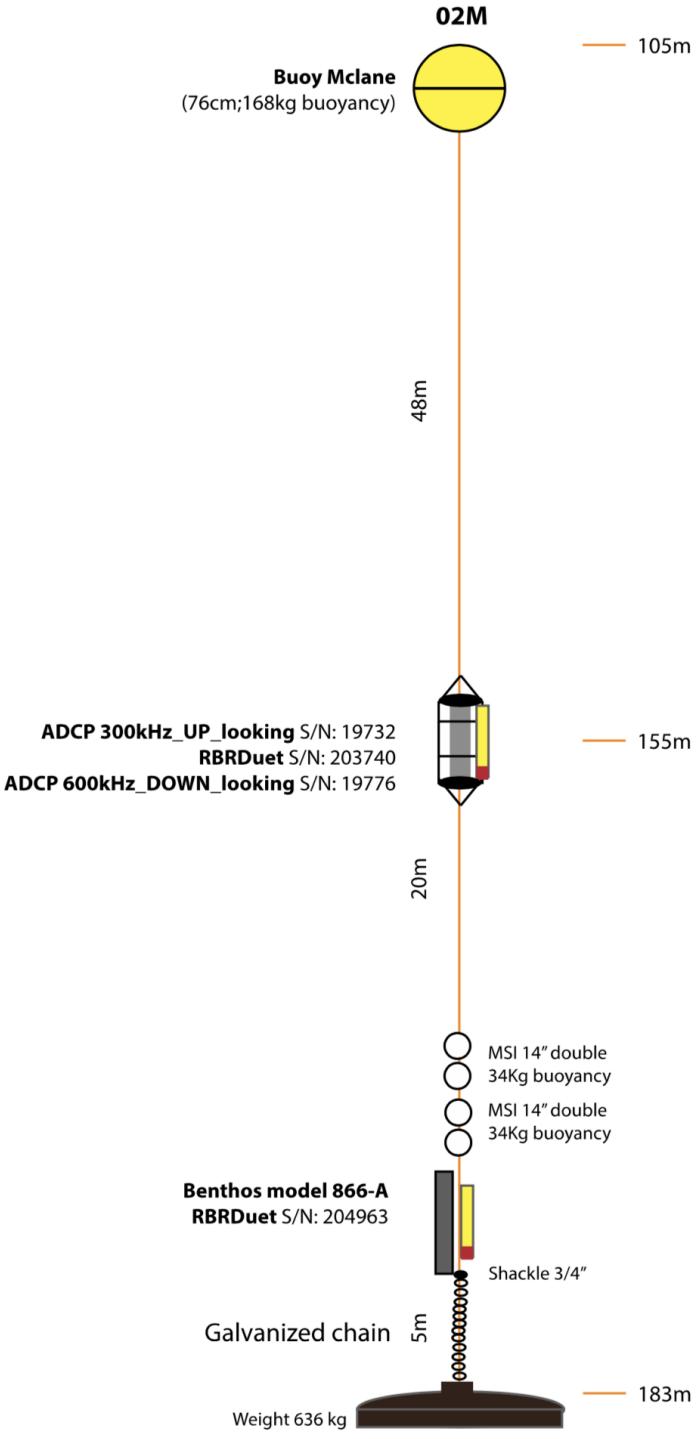

Figure 4: Mooring configuration with depths below water surface.

1.5.2 Waves and weather data

The significant surface wave heights, mean wave period and mean wave direction were obtained with an ADCP, model Nortek AWAC-AST 600 kHz, which was in shallow depth at Pointe-des-Monts and the canyon head (49°18.837' N, 67°21.160' W, depth below mean sea level 39.7 m). Hourly atmospheric measurements of wind speed, wind direction, and air temperature were obtained from the Historical Climate Data of the Government of Canada at the terrestrial weather station Pointes-des-Monts (49°19.20' N, 67°22.80' W, and 5.9 m altitude) which is located at 1.7 km from the mooring. Sea ice conditions were obtained from the daily ice charts produced by the Canadian Ice Service (https://iceweb1.cis.ec.gc.ca/Archive) (Canadian Ice Service, 2020-2021).

1.5.3 CTD casts

Two cycles of 25 hours (approximately 2 semi-diurnal tidal cycles) CTD (Conductivity-temperature-depth) samplings were done from the R/V Coriolis II in the Pointe-des-Monts canyons. The first sampling was on October 16, 2020 with continuous yo-yo down-up profiles from 12:02 UTC. The second sampling was on October 11, 2021, with one CTD cast every hour from 20:25 UTC. Temperature, salinity, and pressure were collected with a CTD/Rosette system equipped with a Seabird SBE 911 sensor recording at 24 Hz. Details of the station positions and samplings times are shown in Fig. 5.

To remove density reversals, the raw density data were sorted into gravitationally stable profiles and the salinity and temperature were reordered following the procedure described in Galbraith and Kelley (1996). To reduce the noise, temperature, salinity, and density data were then averaged into 1 m bin size. The time series of temperature and salinity were linearly interpolated through a vertical resolution of 1 m at 60 s time step.

The buoyancy frequency (N) was calculated to characterize the water column stability,

$$N = \sqrt{-\frac{g}{\rho_o}\frac{\partial \rho}{\partial z}} \tag{1.1}$$

where ρ_o is the reference density (1027 kg m^{-3}), z is the vertical axis positive upward and $g = 9.81$ m s^{-2} is the acceleration due to gravity.

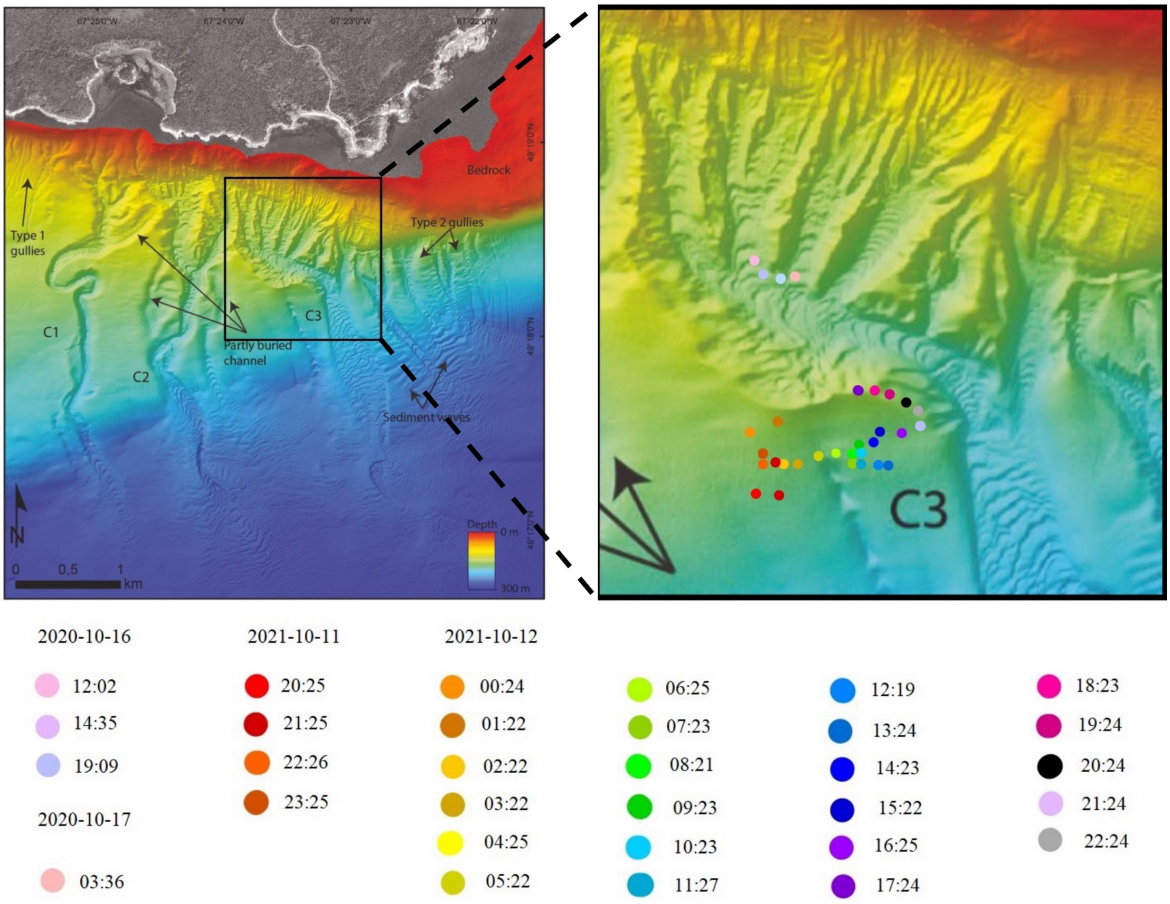

Figure 5: Position of the R/V Coriolis II during the repeated CTD profiles

1.6 Observations and results

1.6.1 Water column structures

The vertical distributions of temperature, salinity, and buoyancy frequency (N) in time-depth space over 2 semi-diurnal tidal cycles are shown in Fig. 6. The CTD data show a stratified water column with strong surface-to-bottom differences in temperature (1.1 °C to 5.7 °C) and salinity (28.1 PSU to 34.1 PSU) in October. The water column is vertically stratified into three layers. The upper layer is 40 m thick and is the warmest with temperature values between 3°C and 5.5°C and the least saline (below 31 PSU). The coldest layer is located at mid-depth between 40 and 100 m where the temperature drops gradually below 1.5°C. In the deepest layer (below 100 m), temperature reversals are clearly observed, the temperature increases with depth and varies between 2.5 °C and 4.5°C. This deep layer is the most saline (above 33 PSU).

The T-S diagram clearly shows three water masses with the mass at intermediate depth characterized by a minimum temperature, which is in good agreement with the knowledge of the water mass in the study region during summer and fall (Fig. 7). In previous studies, the mid-layer is called the cold intermediate layer (CIL) (e.g. Galbraith 2006).

Changes in temperature and salinity stratification throughout different semi-diurnal tidal phases are clearly observed in the central and deepest part of the water column. In the deepest part, the temperature and salinity fields show vertical displacements of up to 50 m with a period close to that of the semi-diurnal tide (12.4 h). For example, during the flood tide beginning at 12:15, October 16, 2020, the lower water column contains more saline and warmer water (around 34 PSU and above 5.5°C), but it is less saline (32.5 PSU) and colder (1.5°C to 3°C) during the following high tide and ebb tide.

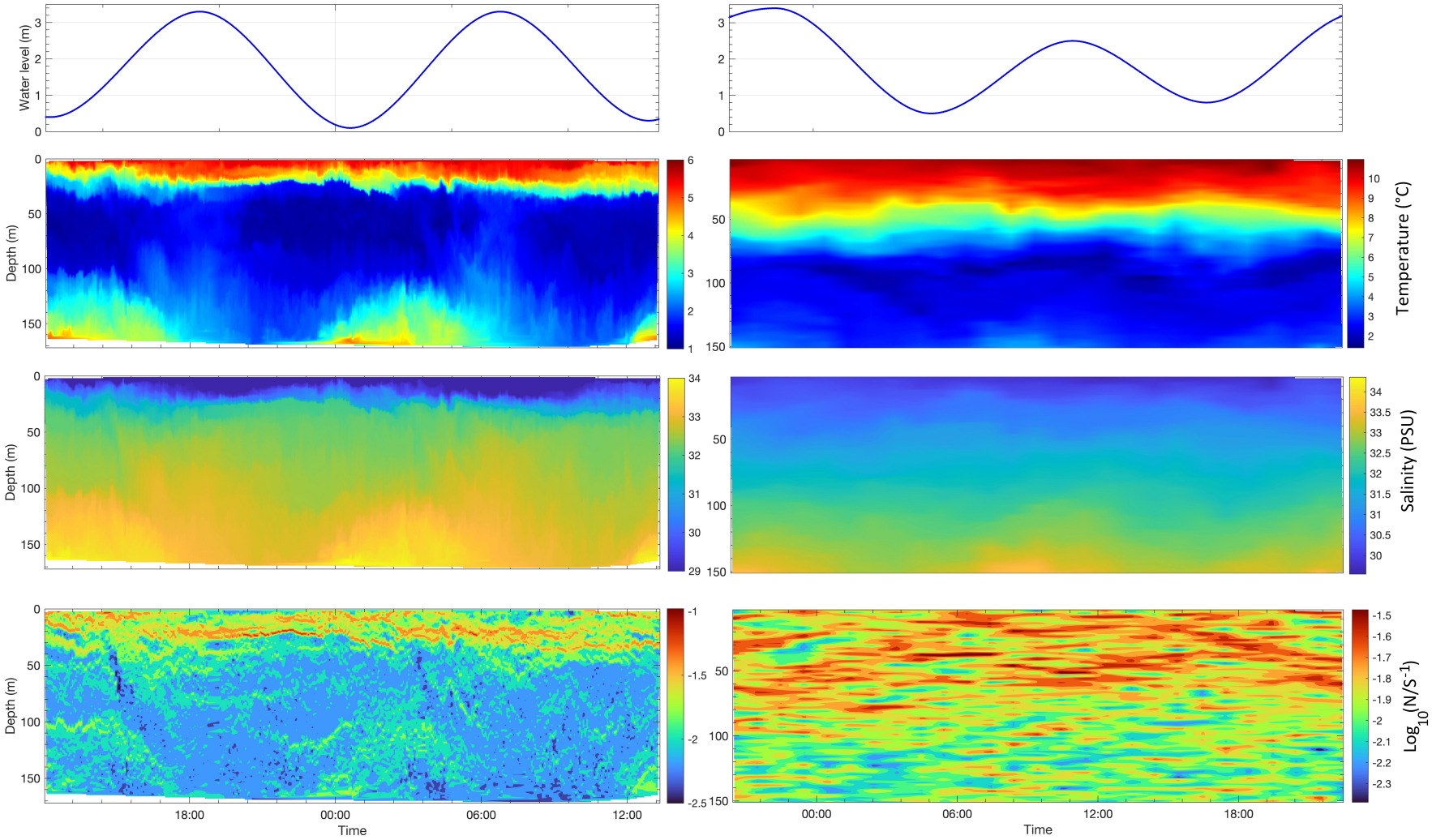

Figure 6: Water level and interpolated temperature, salinity, and buoyancy frequency during two semi-diurnal tidal cycles. The left-hand panels represent continuous down-up profiles on October 16-17, 2020, the right-hand panels hourly profiles on October 11-12, 2021.

These oscillations are interpreted here as internal tides as they have the same semi-diurnal tide period (around 12.4 hours) (Therriault and Lacroix, 1976). The internal (baroclinic) tide is a tide arising from the interaction of the barotropically forced, stratified fluid with a bathymetric obstacle. In contrast to the barotropic tide, the baroclinic component contributes relatively little to oscillations of the sea surface although they have a large internal amplitude (Cummins and Oey, 1997). The CIL also presents vertical displacements and temperature fluctuations. Its thickness decreases and sometimes disappears as the result of the pinching of the CIL by the internal tide (Cyr et al., 2015). These semi-diurnal internal tides are potential interior and boundary mixing mechanisms, which mainly contribute to the erosion of the St. Lawrence CIL as documented in Cyr et al. (2011). The average depth of this layer is approximately 70 meters, and it changes throughout the tidal cycle.

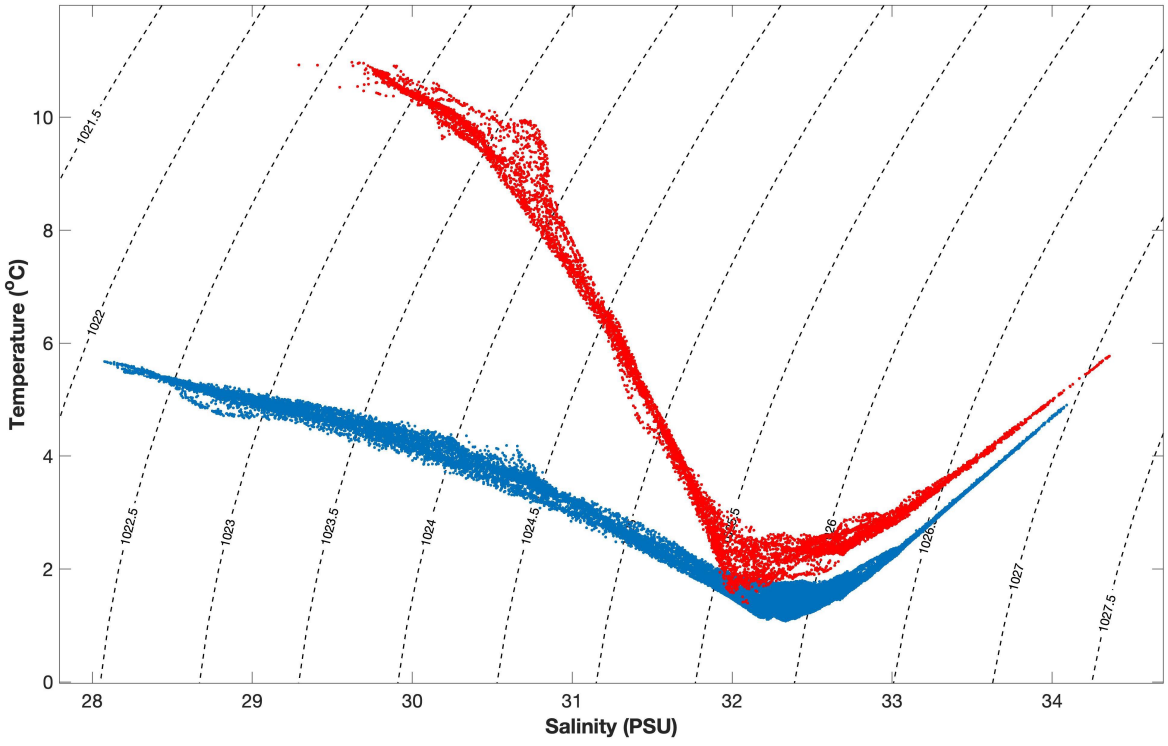

Figure 7: Temperature-salinity diagram showing lines of constant density. (Blue: October 16-17, 2020, Red: October 11-12, 2021)

The mean vertical profiles of two cycles of 25 hours of CTD sampling (Fig 8) show that the temperature exhibits a gradual decrease with increasing depth from 0 to 40 meters in 2020. Similarly, in 2021, the temperature follows a similar trend, but the depth range extends to 80 meters before subsequently increasing with depth. Conversely, the salinity demonstrates an increasing pattern as depth increases, with the steepest gradient between 0 and 40 meters in 2020. These strong temperature and salinity gradients result in strong vertical density gradients (Fig. 8c) and high buoyancy frequencies (Fig. 8d). For 2020 data, the peak water column buoyancy frequencies occurred over a wide range of depths (4 m to 20 m depth) with mean values between 0.029 and 0.035 s^{-1}.

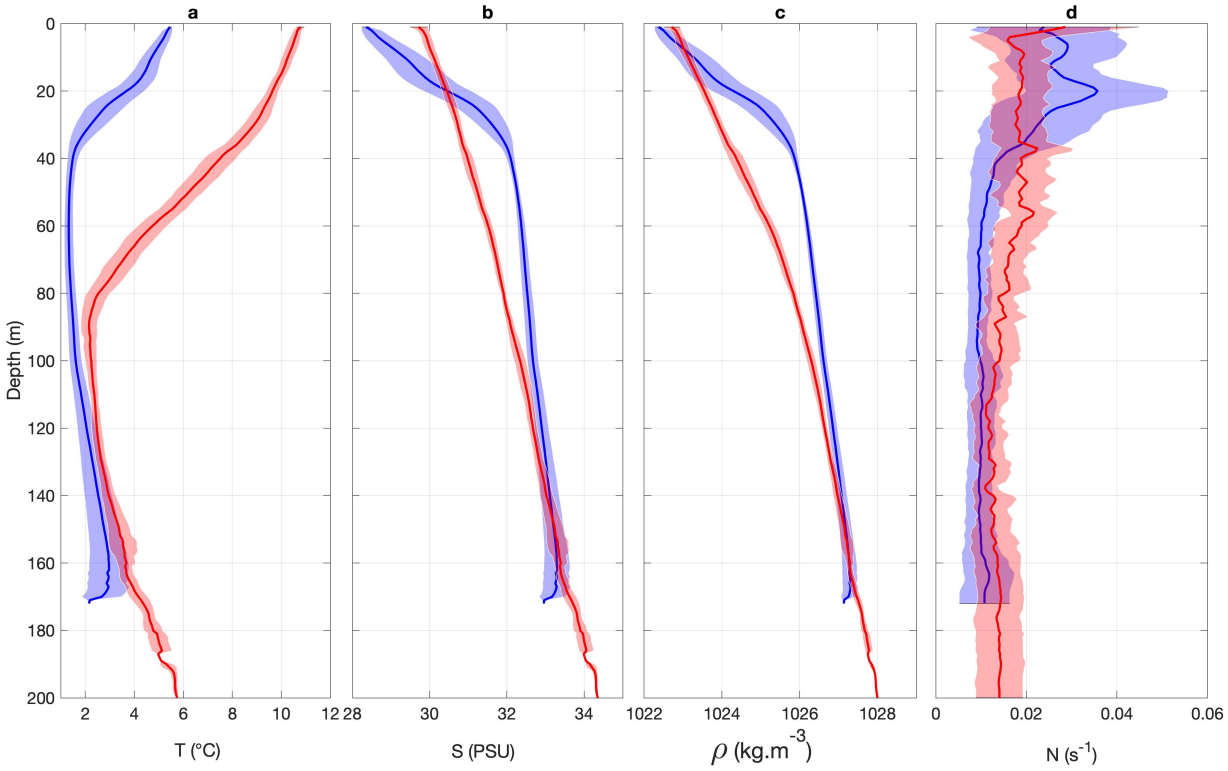

Figure 8: Mean profiles over 25 hours of CTD profiles of (a) temperature, (b) salinity, (c) density, and (d) buoyancy frequency. The shading is ±1 standard deviation. Blue: October 16-17, 2020, Red: October 11-12, 2021.

The near-bottom temperature (at 5 mab and at 27.5 mab) recorded by the mooring dur-

ing one year ranged from 1.5 to 6.3°C and oscillated mainly at semidiurnal tidal frequencies (Fig. 9). The spring–neap cycle is also seen in the temperature time series. The harmonic analysis indicates that the M2 tidal constituent exhibits the largest amplitude (0.23 °C amplitude) followed, in order, by the S2 (32.5% as large as M2), O1, and K1 constituents (Table. 1).

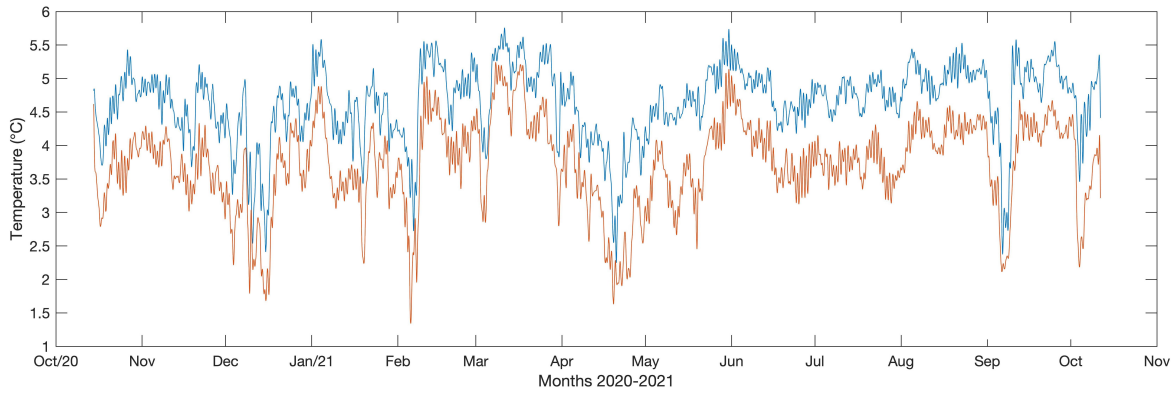

Figure 9: Time-series of the near bottom temperature during the mooring deployment period. Temperature at 5 mab is in blue and temperature at 27.5 mab is in red.

Table 1: Tidal constituent of the near bottom temperature at 5 mab.

Tide	Amplitude (°C)	Phase (°)
M_2	0.236 ± 0.034	28.25 ± 8.77
S_2	0.076 ± 0.035	72.17 ± 24.81
O_1	0.068 ± 0.012	101.18 ± 10.48
K_1	0.051 ± 0.015	139.70 ± 16.47

Tidal temperature oscillations were generally ~ 1.5°C (Fig. 10) with a gradual increase when currents were directed down-canyon and a gradual drop associated with the shift to the up-canyon flow in each tidal cycle. Larger drops in temperature (> 2°C) were observed

occasionally, mainly during periods of cold air temperatures (Fig. 11). The sharpest drops in temperature (4°C) were observed during the winter and fall season.

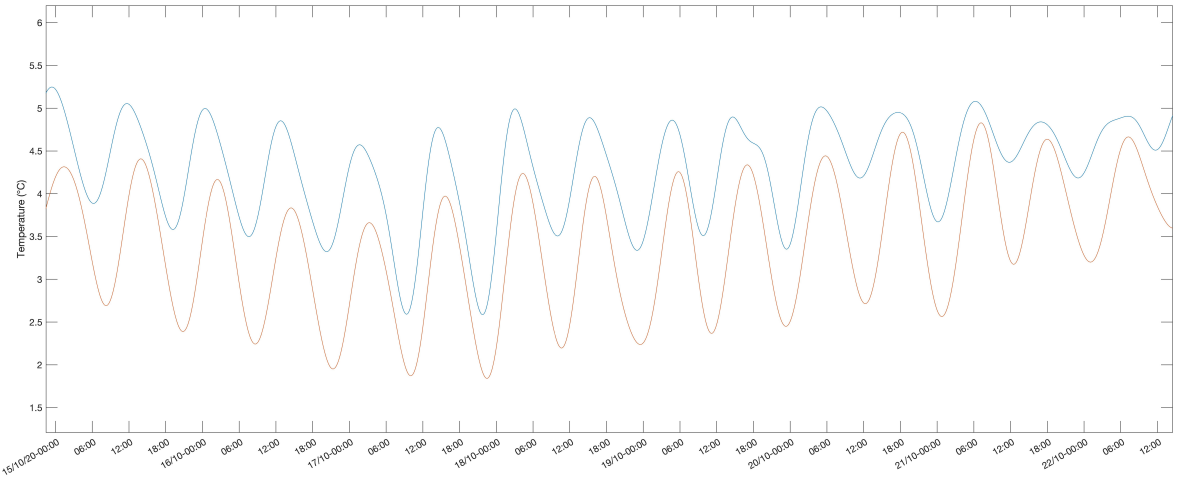

Figure 10: Exemple of near bottom temperature variation with tides. Temperature at 5 mab is in blue and temperature at 27.5 mab is in red.

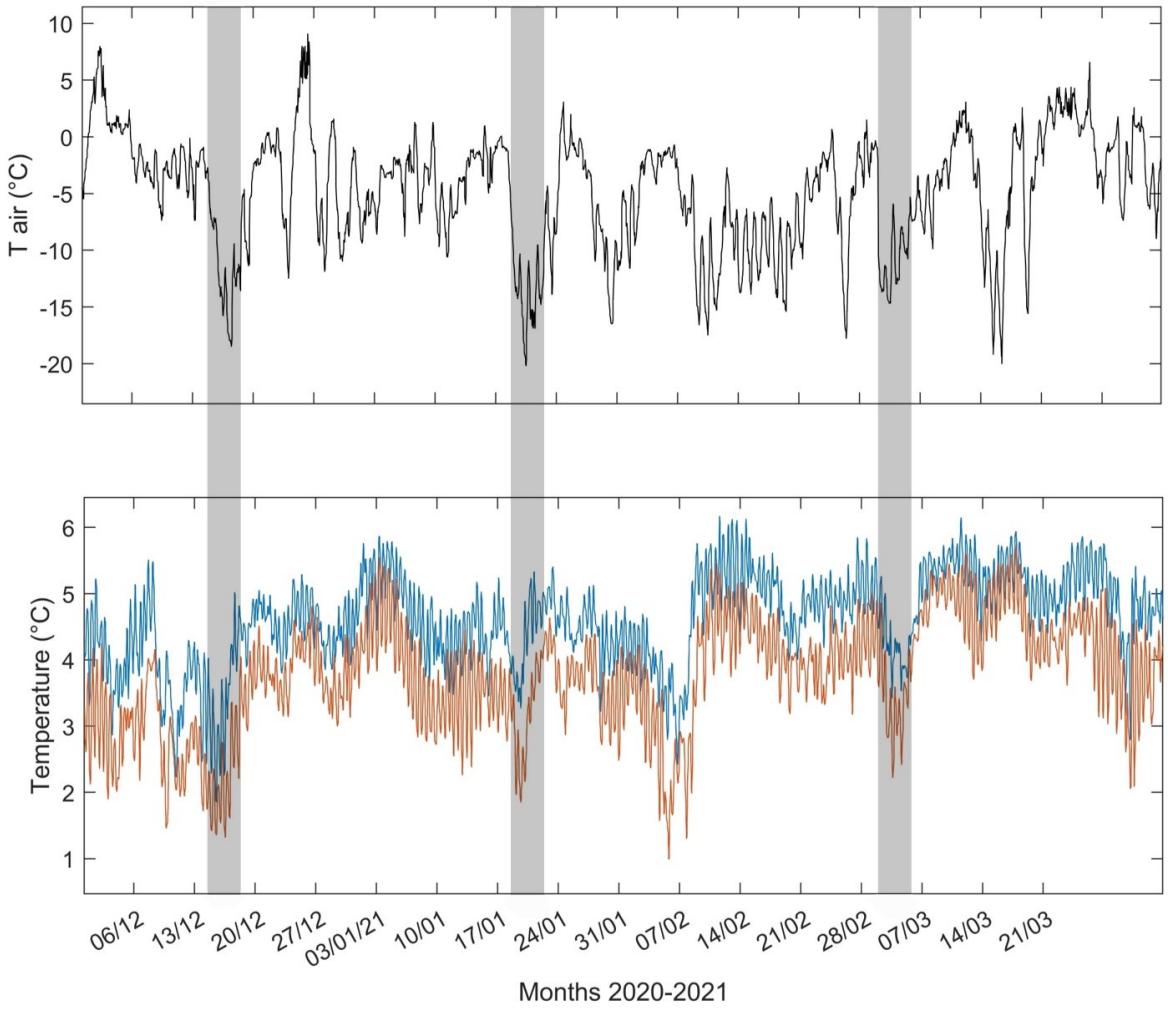

Figure 11: Air temperature and near bottom temperature variation. Temperature at 5 mab is in blue and temperature at 27.5 mab is in red.

1.6.2 Near-bottom currents

A rose diagram of the 0-26 mab vertically-averaged current was constructed to synthesize the direction and intensity of the current. The current rose shows that the currents were mainly oriented along the west-northwest east-southeast axis which is the same direction as the main canyon's axis (Fig. 12). No significant seasonal variation in the near-bottom hori-

zontal current direction was noticed (Fig. 13). This orientation was then used to create the axis system in Fig. 3. The u and v velocities (respectively eastward and northward velocity components) were rotated over a –22 ° rotation angle (α) from the east-north axis system according to

$$u_r = u\cos(\alpha) - v\sin(\alpha) \tag{1.2}$$

$$v_r = u\sin(\alpha) + v\cos(\alpha) \tag{1.3}$$

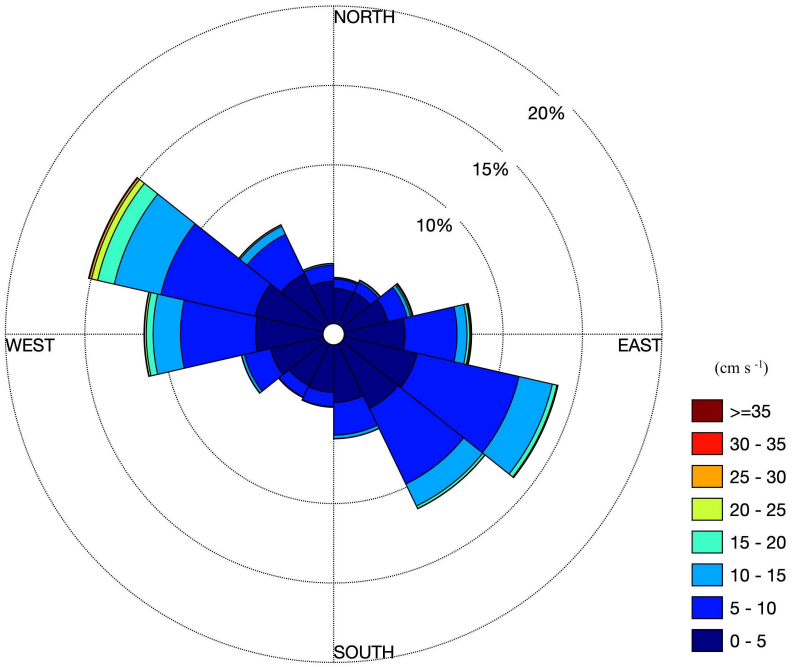

Figure 12: Current rose of the 0-26 mab vertically-averaged current for the entire deployment.

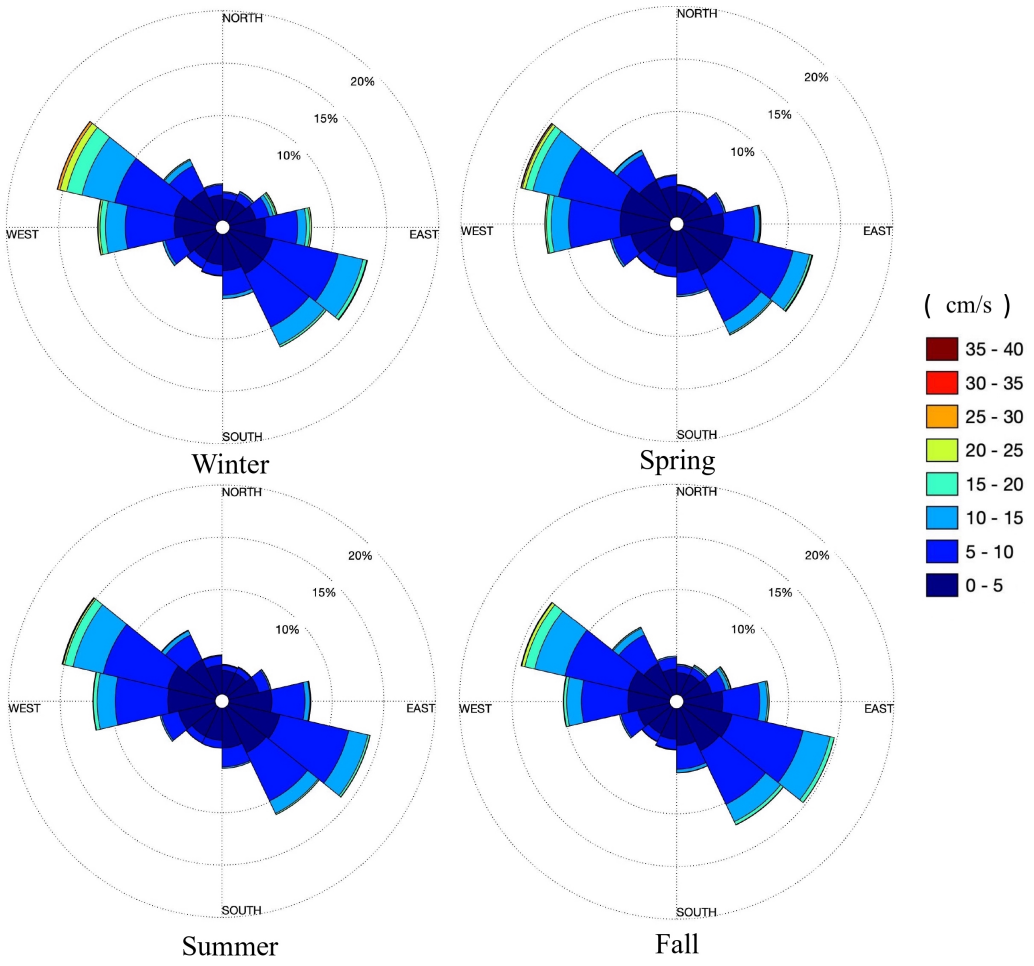

Figure 13: Current roses of the 0-26 mab vertically-averaged current for the different seasons.

Figure 14 displays a 3-day detail of the near-bottom horizontal currents. The current flowing along the canyon (u_r) is larger than the across-canyon current (v_r). Currents fluctuated at semidiurnal tidal frequencies (u_r component shows stronger semi-diurnal signal). A vertically-averaged current (0-26 m) was calculated to characterize the near-bottom currents.

The yearly mean of the magnitude of the near-bottom horizontal velocity components are $|u_r|$ = 5.1 ± 6.6 cm/s (mean ± standard deviation) and $|v_r|$ = 2.4 ± 3.1 cm/s. The yearly mean of the horizontal velocity magnitude is $|U_r|$ = 13.4 ± 2.8 cm/s. The yearly mean of each velocity component are u_r = -0.47 ± 5.14 cm/s and v_r = 0.14±4.23 cm/s, which shows a

residual up-canyon flow of 0.49 cm/s towards the northwest.

The yearly mean bottom horizontal velocity magnitude at 1 mab is $|U_{r1}| = 15.77 \pm 8.45$ cm/s. During periods of normal conditions, u_r and v_r velocities magnitude were $> \pm 25$ cm/s between 0 and 10 mab with higher velocities being recorded during up-canyon flows. High current velocities were observed in the records, with the highest horizontal bottom current speed $|U_{r1}| = 85$ cm/s recorded during a turbidity current event in February 2021.

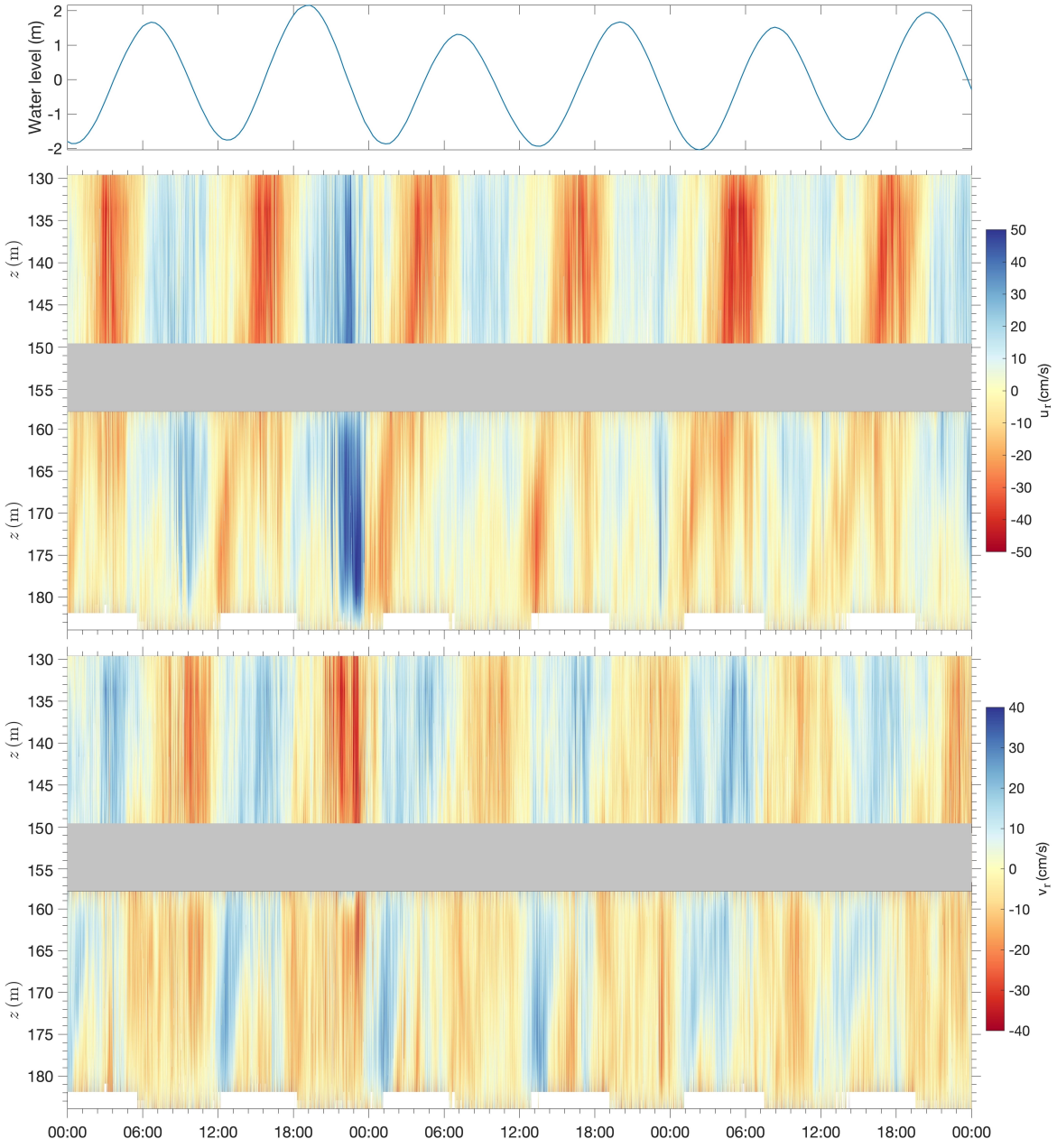

Figure 14: Three-day (17, 18 and 19 October 2020) detail of water level above mean sea level and horizontal currents u_r and v_r measured by the 2 ADCPs. The vertical scale is depth below sea surface. The grey area represents missing data between the two ADCP datasets and data that have been eliminated due to their poor quality.

1.6.3 Velocity Structure

The residual velocity, after tidal and inertial signals were removed with a 15-day low-pass filter, are shown in Figure 15 with the u_r component (along canyon axis) and the v_r component (cross canyon axis) for the entire deployment period. The horizontal residual current velocity is almost constant during the whole year, with no significant seasonal change observed in the bottom water column, where the effect of the surface wind and waves is negligible. As expected, the along-canyon velocity is more energetic than the across-canyon velocity ($\sim$ 1.2 cm/s). For the v component, the strongest magnitude was observed throughout the entire year between 2 m and 8 m above the seabed.

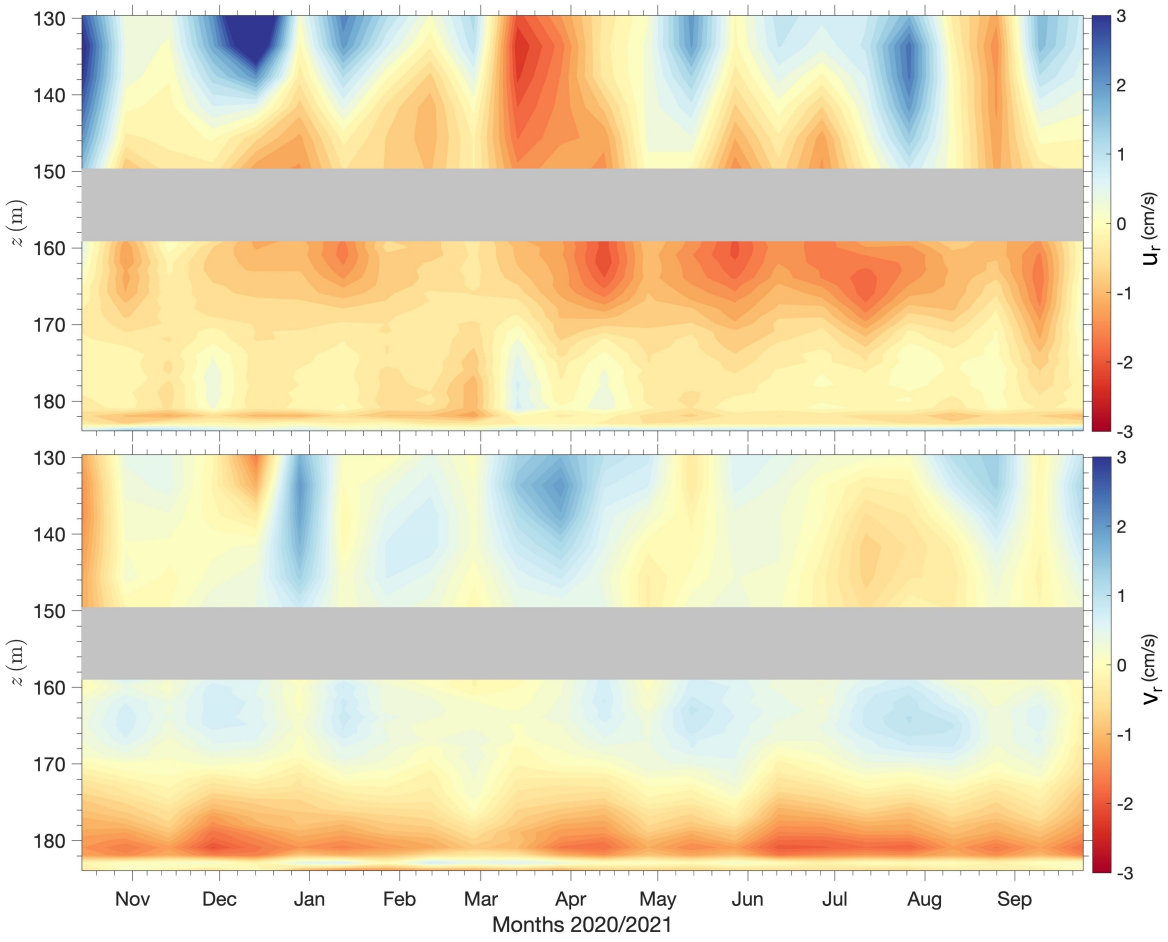

Figure 15: 15-day low-passed velocity components u_r (top panel) and v_r (bottom panel) throughout the entire deployment period. The vertical scale is depth below sea surface. There are no data between 150 an 159 m because of the blanking distances of the two ADCPs.

1.6.3.1 Power spectra

To examine the energy distribution over the frequency range, a spectral analysis was performed on the pressure and temperature recorded by the RBR mounted at 5 mab, and the vertically-averaged horizontal current recorded by the down-looking ADCP (Fig. 16). As expected, the horizontal current, water temperature and pressure are primarily influenced by the semi-diurnal tidal constituents M2 (highest peak, 12.42 h, 1.93 cpd) and S2 (12 h, 2.00

cpd), and secondarily by the diurnal constituents O1 (25.82 h, 0.93 cpd) and K1 (23.93 h, 1.00 cpd). In addition, numerous other tidal components are clearly seen, including peaks at the M3, M4, and M6 frequencies in the power spectra of the horizontal current and the pressure, but with lower energy levels. There is no indication of relatively high-energy motion within low-frequency bands. No distinct peak in the frequency spectrum is seen at the inertial frequency f (1.52 cpd) for this particular latitude.

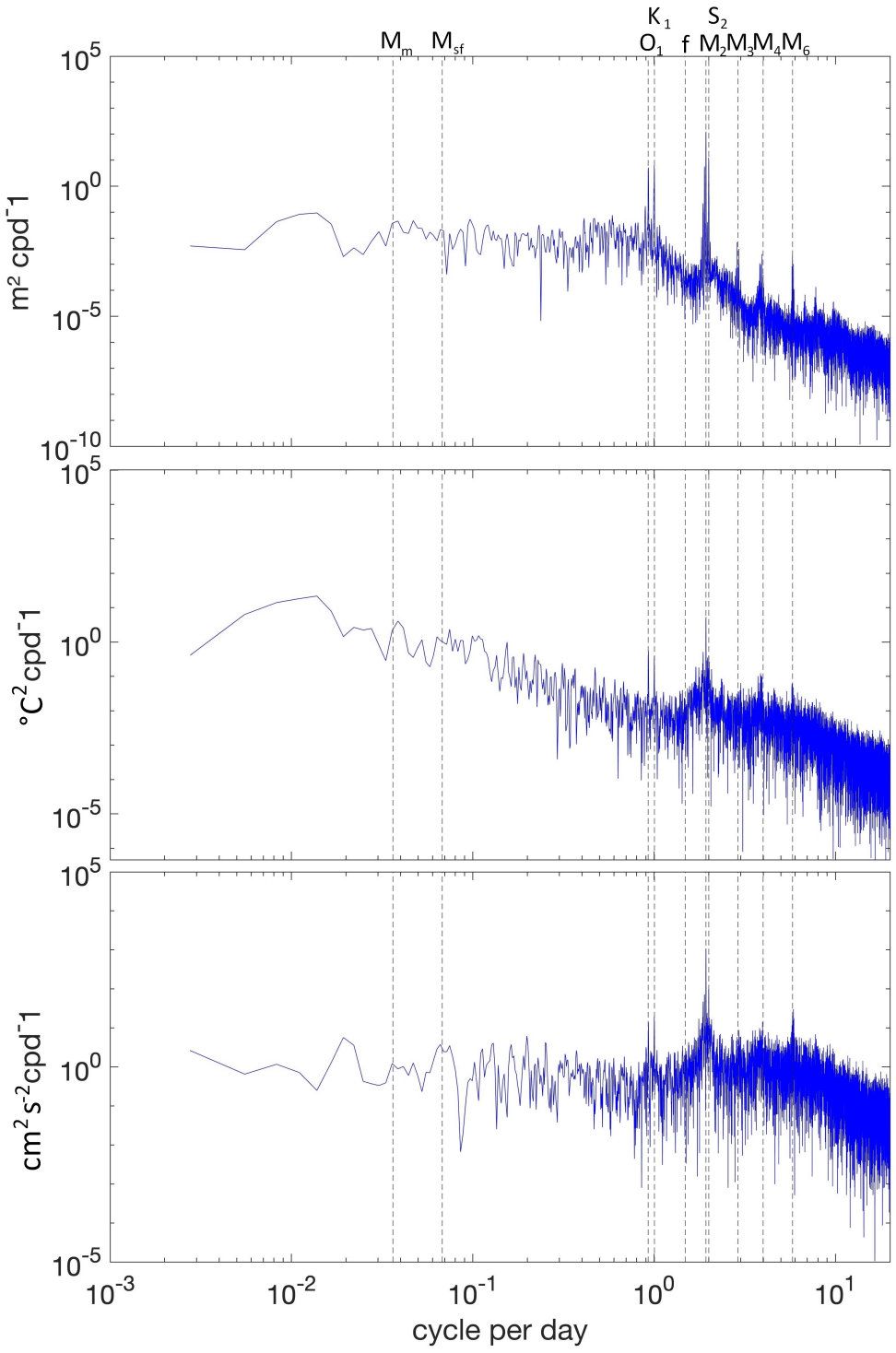

Figure 16: Power Spectral densities of the water level (top), temperature at 5 mab (middle), and the vertically averaged current (0 - 26 mab) in the canyon axis direction (bottom). Labels were given to single peaks at tidal constituent frequencies.

1.6.3.2 Tidal analysis

In order to characterize the frequency content and variability of the tides, a tidal analysis resolving 16 different tidal constituents was performed on the vertically averaged horizontal current recorded by the down-looking ADCP. The obtained results are summarized in Table 2. This analysis reveals that the strongest constituent for the velocity is the M2 tide, as for the temperature time series. The major semi-diurnal harmonic ellipses (M2, S2, N2) were oriented to the east-southeast at 112°, whereas the other constituents were slightly off from that angle. This orientation is consistent with the results of the wind rose analysis shown in Fig. 12.

Table 2: The 16 most important tidal constituents of the vertically averaged 0-26 mab current. The angle is the direction of the major axis relative to the north. The phase is relative to Greenwich. The sign of the minor axis indicates the sense of rotation of the tidal current vector, which is positive for cyclonic rotation and negative for anti-cyclonic rotation.

Name	Major axis (cm/s)	Minor axis (cm/s)	Angle (°)	Phase (°)
M_2	4.41±0.181	-0.945±0.130	112±1.6	197±2.9
S_2	1.29 ±0.183	-0.371 ±0.129	109±5.5	255± 9.5
N_2	1.19±0.196	-0.223±0.119	112± 5.9	189± 10.1
$2MS_6$	0.809± 0.141	-0.127±0.0872	108±6.6	205± 9.2
M_4	0.802±0.121	0.0821±0.0712	141±5	242± 11.4
MU_2	0.718±0.216	-0.0509±0.114	104±10.6	205±14.8
M_6	0.652± 0.124	-0.139±0.0786	109±7.4	160±12.4
K_1	0.584±0.0815	-0.0680± 0.055	121±6.4	233±6.8
O_1	0.532± 0.0741	-0.0721± 0.056	117±6.2	206± 7.5
MS_4	0.272± 0.160	0.107±0.0757	143±23.5	244± 40.3
H_2	0.199± 0.109	-0.138±0.172	36.9±122	314±88.0
Lda_2	0.214±0.170	0.0421± 0.117	104±32.6	95.4±50.7
MM	0.165±0.0847	0.0448±0.116	90.6±47.1	249±38.3
MSF	0.129±0.0877	0.0417±0.0832	128±49.9	274±56.5
$2MK_6$	0.206±0.205	0.002±0.12	101±35.7	192±70.7
NU_2	0.171±0.295	0.004±0.17	98.29±46	205±137

1.6.4 Sediment transport processes

The analyses of the backscatter and velocity data collected by the ADCPs suggest two main sediment transport processes acting on the head of Pointe-des-Monts canyons. The first occurs during periods of moderate bottom current velocities in up-canyon direction, which

are presumably caused by internal tidal bores. The second is associated with down-canyon turbidity currents occurring during storms with strong wind, high waves, and cold air.

1.6.4.1 Internal tidal bores

Regular occurrences of what appear to be internal bores were noticed during the analysis of the current measurements in the canyon axis direction. These internal bores consist of sudden passages of internal fronts suspected to be unstable and breaking. They are comparable to tidal bores that form on tidally-energetic rivers, but they are generated internally. Figure 17 displays three examples of such internal bores. These bores are characterized by upslope horizontal currents of order $u > 10$ cm/s and are accompanied by an increase in backscatter intensity, starting at the seabed and progressing up to 15-20 mab. This increase in backscatter intensity likely indicates resuspension of fine sediment, which can then be transported toward the canyon head by the currents associated with the bore.

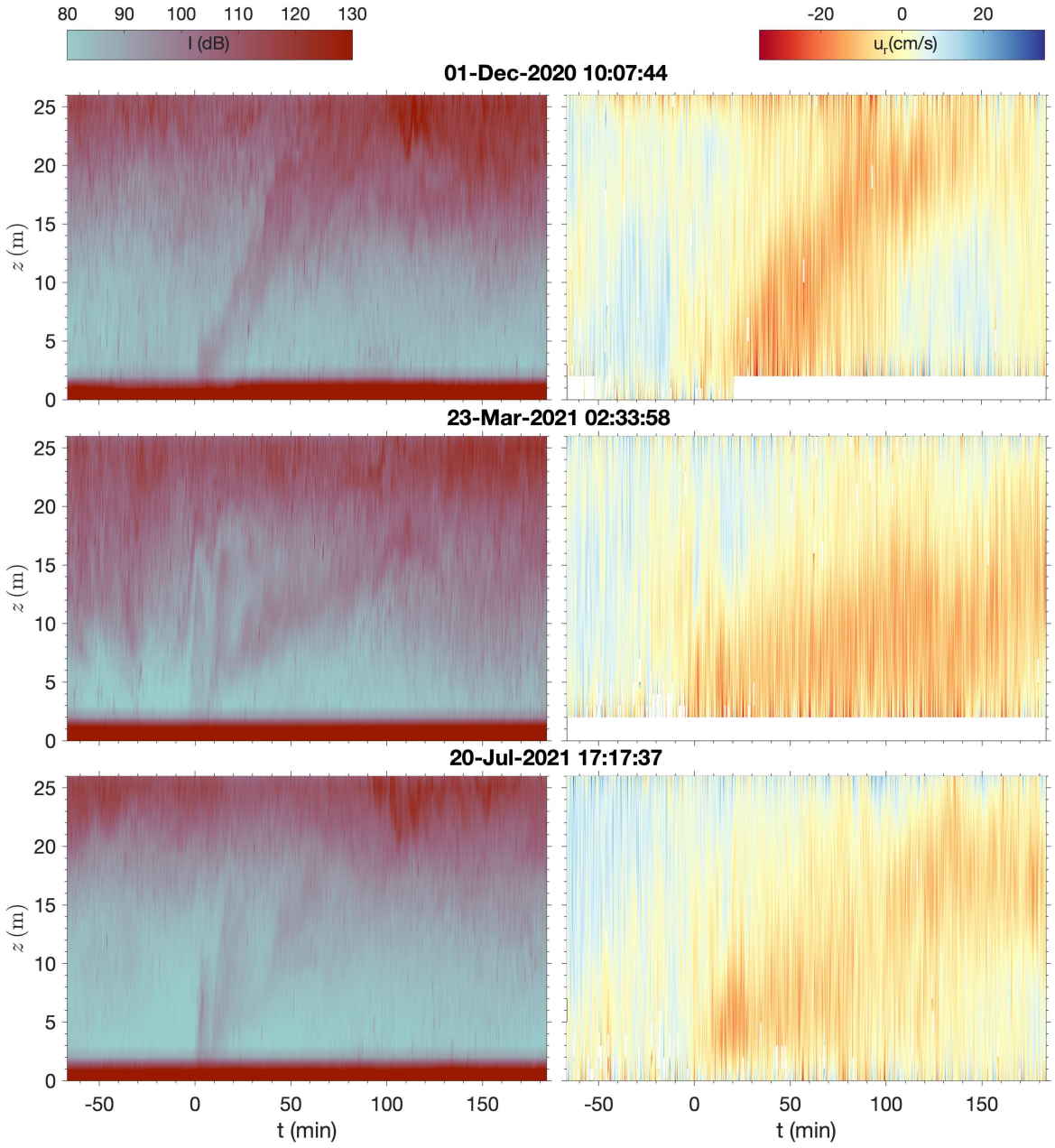

Figure 17: Three examples of internal tidal bores. (Left) Backscatter intensity (I). (Right) Velocity along the canyon axis (u_r, positive down-canyon).

Over the 362 days deployment, 532 similar features were manually identified, which corresponds to an occurrence frequency of 536 bores/year. Figure 18 shows the velocity and

backscatter structures averaged over the 532 identified bores, where $t = 0$ corresponds to the bore front. These bores are typically characterized by a maximum horizontal velocity of 15 cm/s and a vertical velocity of 1.5 cm/s.

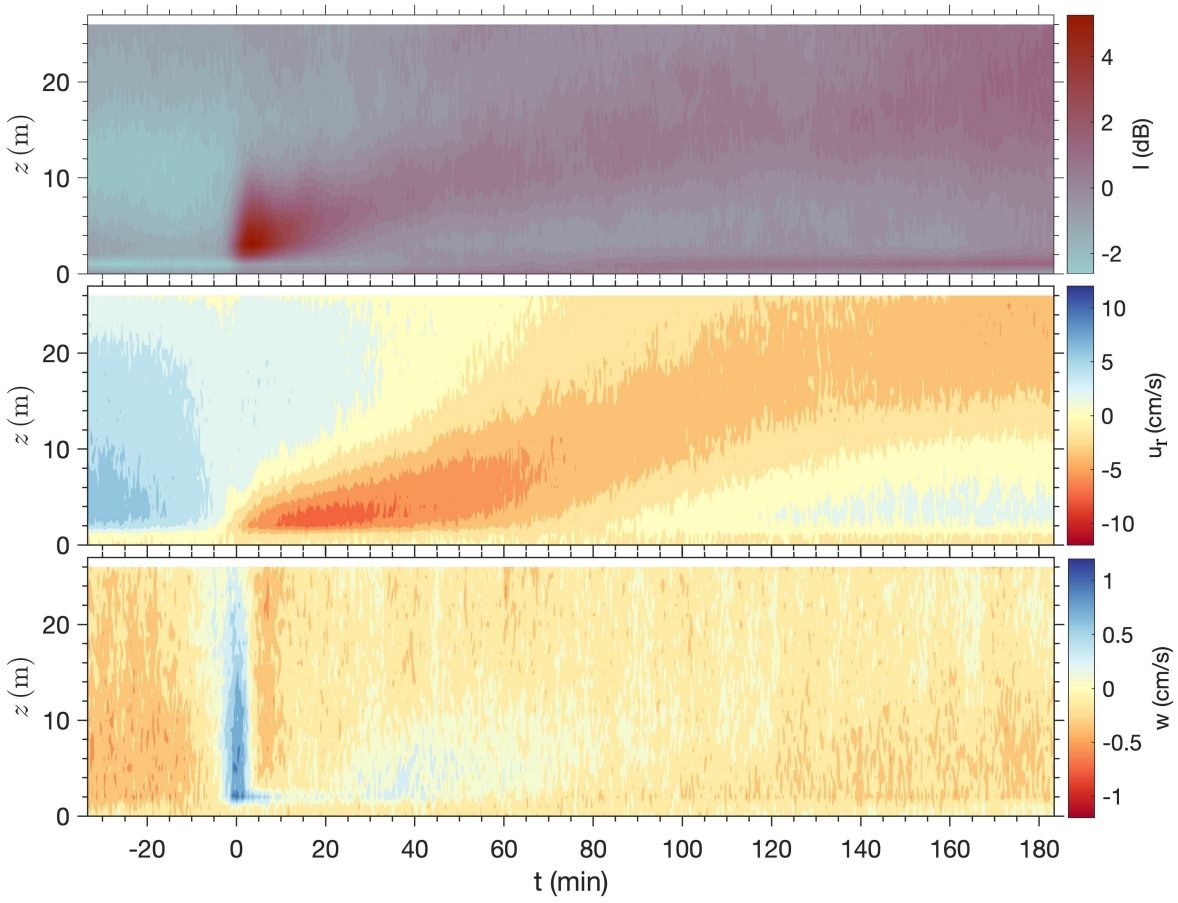

Figure 18: Ensemble average of the backscatter (I), horizontal current (u_r, positive down-canyon), and vertical current (w) structure of the 532 bores identified.

To investigate a possible relationship with the baroclinic tidal signal, the timing of the bores relative to the internal tide level determined through near-bottom temperature was examined. For the entire deployment, the onset of each bore was visually identified in the backscatter record. The results show that these internal bores have the highest occurrence probability ($> 70\%$) centered at 1.0 ± 0.5 h after the time of low internal tide, but they are

also found at other phases of the semi-diurnal tidal cycle (Fig. 19). The probability of finding these bores decreases on each side of this centered value to become less than 1% for the hour of high internal tide. The time difference between successive internal bores varied between 12.3 and 111 hours but 73 % fell between 12 and 25 hours. The average time interval between a bore passage and the previous surface high tide is 3.6 h with a maximum of 9 h, a minimum of 1.7 h, and a standard deviation of 0.8 h. The period during which the sediments remain suspended has an average of 2.4 h, with a maximum of 2.7 h, a minimum of 1.6 h, and a standard deviation of 0.6 h. Internal tidal bores occur during both spring and neap tides and are not correlated with any particular season.

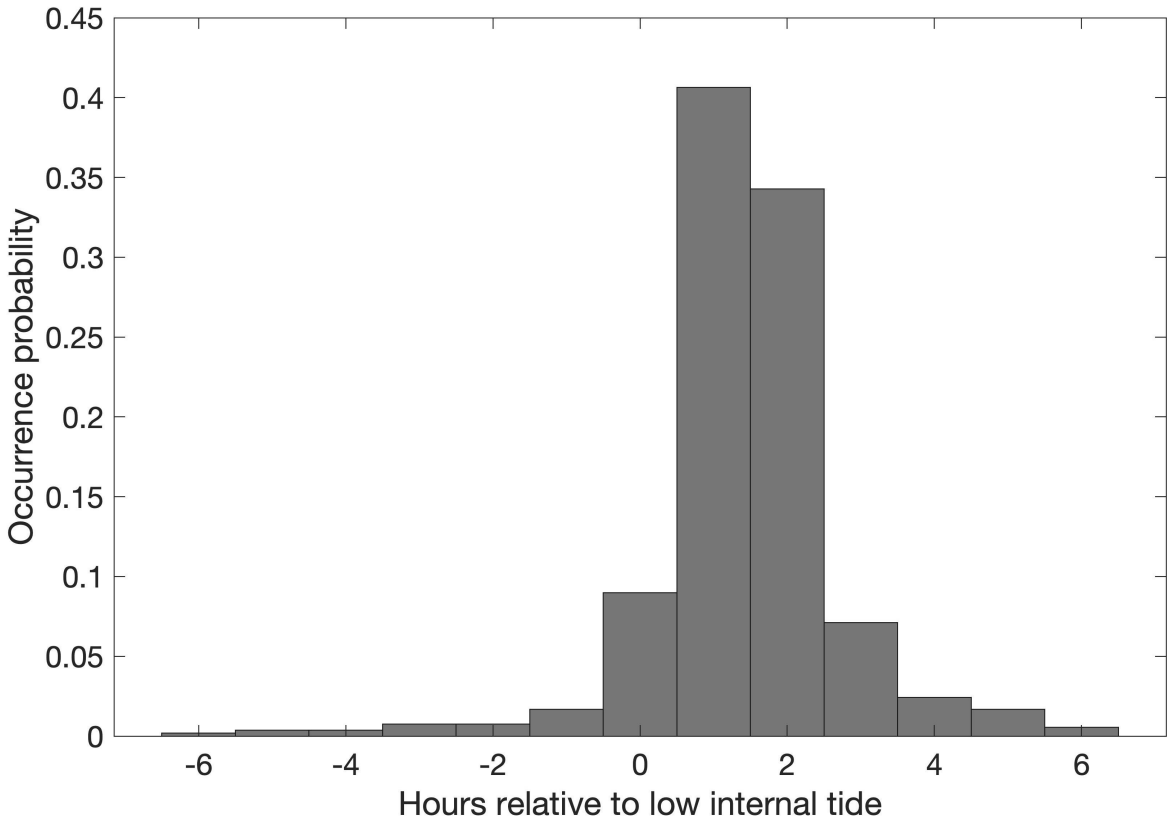

Figure 19: Histogram of the internal bore occurrence probability relative to the semi-diurnal internal tidal phase.

1.6.4.2 Turbidity current

Combining the observations of backscatter and along-canyon velocity, only one turbidity current was identified by its high values of backscatter signal in combination with a sharp increase in down-canyon velocity. It occurred on the 3rd of February 2021 at 14:57 UTC and lasted over two hours. A detailed view of the backscatter and velocity data is given in Figure 20. This event had the strongest near-bottom backscatter intensity and the fastest bottom currents during the entire one-year deployment.

During the turbidity current event, the horizontal velocity increased from near zero to a maximum down-canyon velocity of 233 cm/s in a few minutes. The highest velocity occurred at the front of the turbidity current, very close to the canyon floor at 3 mab. The high velocity gradually extended upwards in the water column. It is associated with maximum backscatter intensity suggesting maximum sediment concentration. As the turbidity current arrives, the near-bottom water temperature at 5 mab increased from 3.8°C to 4.5°C. There was no rise in the mooring tilt during to the turbidity current's arrival, and no variation in the mooring depth was observed after this event. An important feature of this turbidity current is that it had two distinct pulses. It started with a first pulse with a thin ($<$ 10 m), fast, and dense layer for a short duration (4 min), followed by a second pulse 36 minutes later. The extent of suspended sediment cloud reached a height of more than 26 m. Backscatter intensities then remained higher than normal for a few hours until most sediments settled in the canyon, like in other environments where turbidity currents occur (e.g. Azpiroz-Zabala et al. 2017).

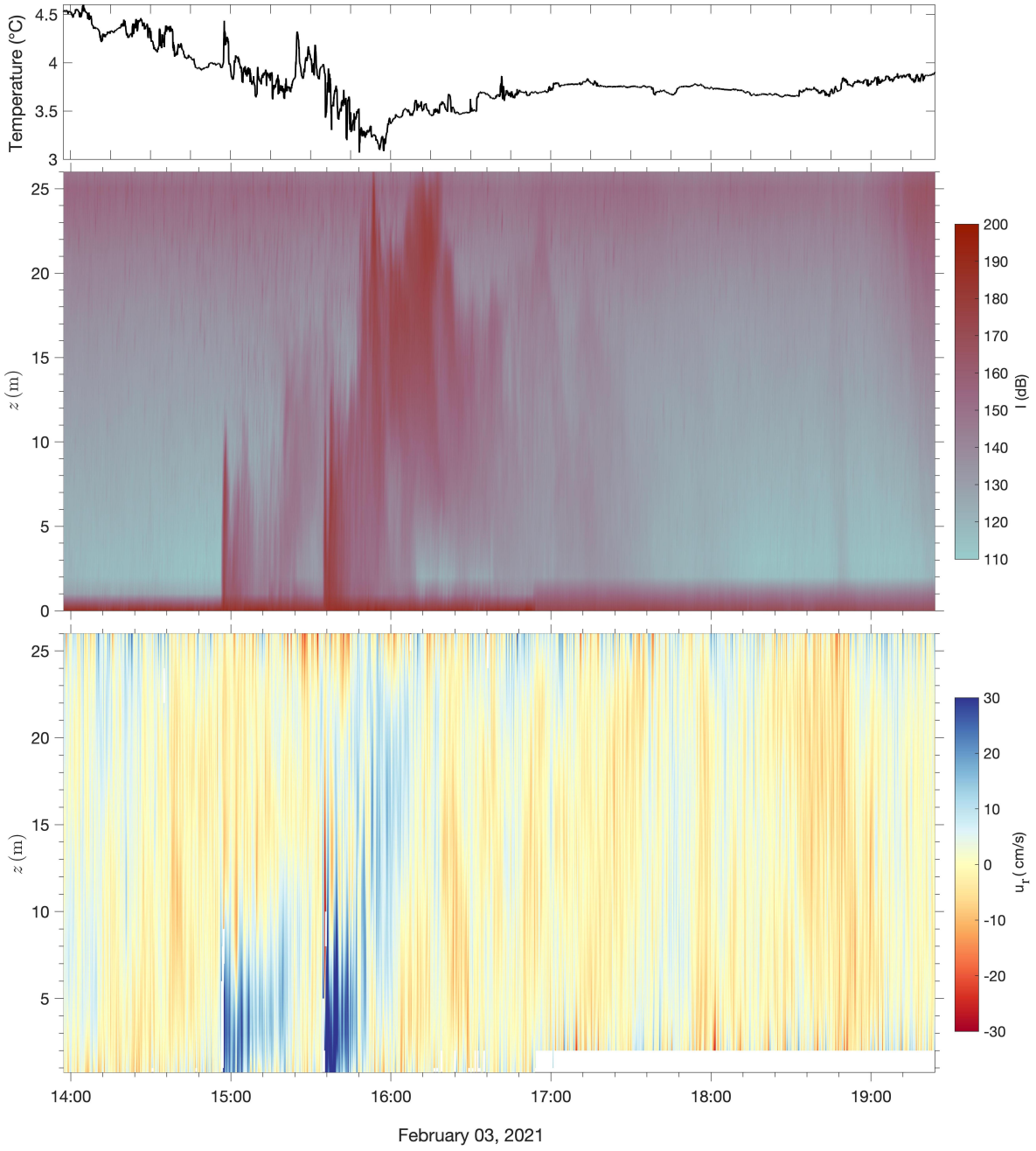

Figure 20: Variation of temperature at 5 mab (top), backscatter intensity (middle), and velocity (bottom) during the turbidity current.

To better understand the potential trigger of turbidity currents in the Pointe-des-Monts

canyons, it is useful to look at environmental variables such as air temperature, wind speed and direction, and waves. This turbidity current was triggered during a storm that hit Pointe-des-Monts with a strong NE wind (> 60 km/h), ENE waves with a significant wave height (H_{m0}) of 4.8 m and a mean wave period (T_{02}) of 7.2 s (wave peak at 13:00, two hours before the turbidity current), and a cold air temperature (−1.5° C; Fig 21). The event occurred during falling surface tide, 3 hours before low tide. The water level was 0.07 m below mean sea-level. There was a storm surge, peaking at +0.77 m 3½ hours before the event, and still at +0.57 cm when the turbidity current occurred. Even if this turbidite happened in the middle of winter, the water surface was ice-free. The fact that the turbidity current didn't occur at the peak of the wave height, but only 2 hours later during the falling tide and 3 hours before the low water suggests two possible explanations. (1) Strong storm waves must last long enough to move enough sediment to the canyon head or (2) relative shallow water depths are necessary on the 200-400 m wide 1-6 deep (below mean sea level) shelf that is in front of Pointe-des-Monts.

Throughout the entire deployment (October 2020 to October 2021), three major storms occurred on 17 January 2021, 03 February 2021, and 27 March 2021 with strong wind speeds (> 60 km/h) and significant wave heights (3.6 m, 4.8 m, 3.0 m, respectively). These storms had a mean wave period of 6.4 s, 7.2 s and 6.1 s, respectively (Table 3). Only the storm that occurred on 03 February 2021 triggered a turbidity current. The other two storms had no effect on bottom velocities and backscatter in the canyon. This suggests that there are other conditions that are responsible for triggering turbidity currents in addition to the storms.

Table 3: Conditions of the three largest storms that occurred throughout the deployment period.

	Storm 17/01/2021	Storm 03/02/2021	Storm 13/03/2021
Wind speed (km/h)	74	60	68
Wind direction	NE	NE	NE
Wave height (m)	3.6	4.8	3.0
Wave direction	E NE	NE	NE
Wave period (s)	6.4	7.2	6.1
Air temperature (°C)	-1.5	-1	-3
Tide	Low	Low	Low
Duration of the turbidity flow (hour)	5	7	4

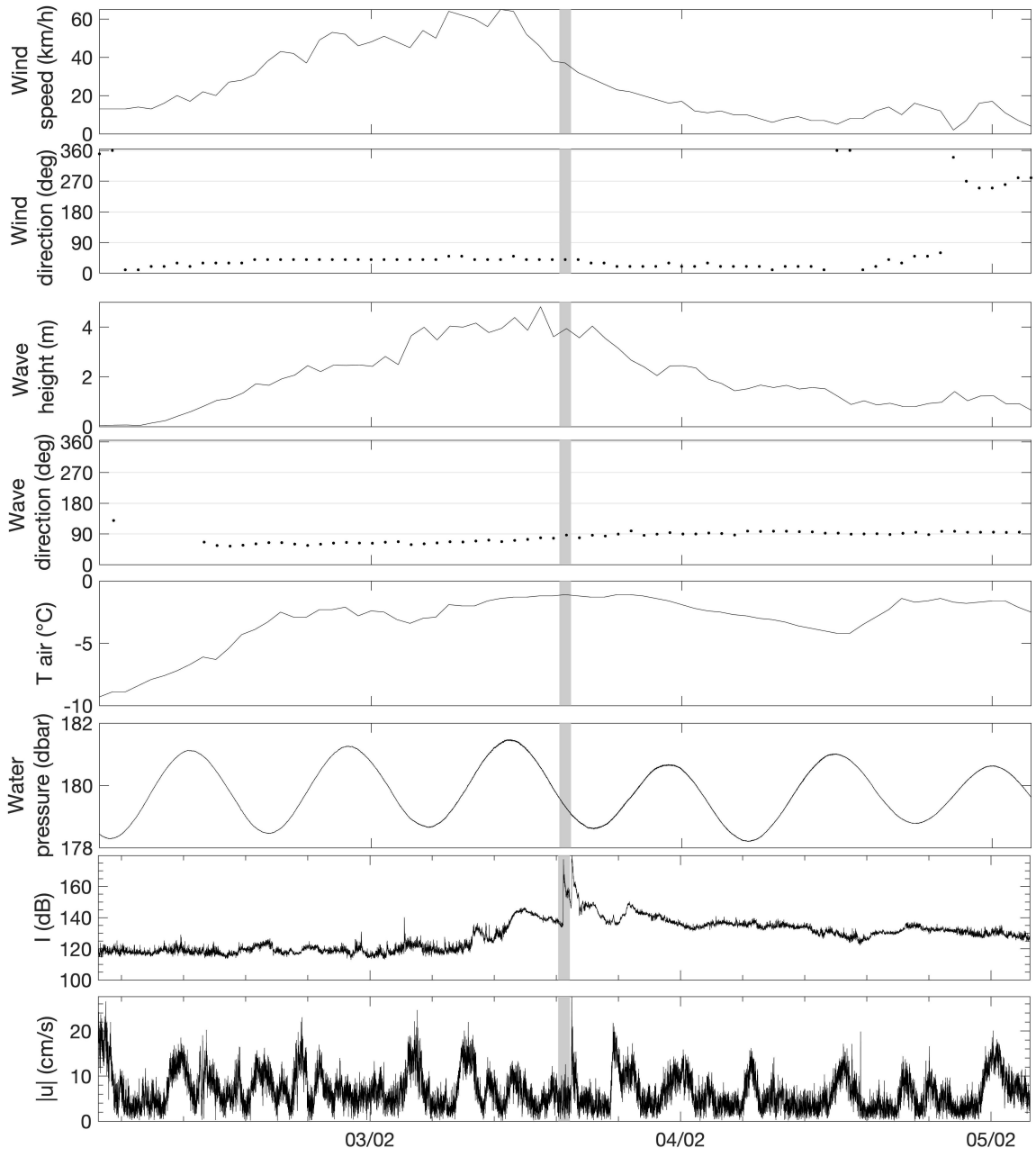

Figure 21: Turbidity current average backscatter and atmospheric conditions (the grey bar marks the time of the turbidity current).

The structure and condition of this turbidity current are comparable to those seen in previous measurements in the Pointe-des-Monts canyons documented in Normandeau et al. (2020). The common characteristic of these turbidity currents is that they all have been triggered during storms with wind speeds > 60 km/h for several hours, important wave height, and at or near low tide (Table 4). Between October 2016 and October 2017, two strong and two weak turbidity currents took place (Normandeau et al., 2020). Only one happened between October 2020 and October 2021 (present study). However, no turbidity current was identified during a deployment from June 2015 to July 2016 (Normandeau et al., 2020). Similarly, no turbidity current was identified in the data of an additional deployment from October 2021 to October 2022, according to the preliminary data analysis. Given these few documented events (two years with no event, one year with one event, one year with two strong and two weak events), still no annual frequency of turbidity current occurrence can be determined for the Pointe-des-Monts canyons.

Table 4: Storm conditions that occurred in Pointe-des-Monts between October 2016 and October 2021.

	Storm 12/11/2016	Storm 04/01/2017	Storm 25/01/2017	Storm 15/03/2017	Storm 03/02/2021
Wind speed (km/h)	76	74	65	81	68
Wind direction	SW	NE	NE	NE	NE
Wave Height (m)	1.0	4.6	4.4	3.8	4.8
Wave direction	SSE	NE	NE	NE	NE
Wave period (s)	4.0	7.0	7.0	6.9	7.2
Air temperature (°C)	-2.1	-2.6	-3	-3.7	-1
Tide	Low	Low	Low	Low	Low
Turbidity current	Weak	Weak	Medium	Strong	Strong

1.7 Discussion

Data collected within the Pointe-des-Monts submarine canyons reveal various physical processes that exist in deep canyons. Internal tides are clearly visible in both temperature and salinity water-column data of the two 25-hours CTD data sets. They are characterized by a large amplitude ($\sim$ 50 m) compared to the surface tide ($\sim$ 3 m). The pronounced oscillations with semi-diurnal and diurnal tidal frequencies found in the near-bottom horizontal velocity and temperature records are also primarily caused by internal tides. The mechanism behind these tidal fluctuations in canyons is the stratification of the water column combined with barotropic tides in regions of variable bathymetry, which induce internal waves of tidal period (Petruncio et al., 1998; Therriault and Lacroix, 1976). As submarine canyons are traps for internal waves (Gordon and Marshall, 1976), the majority of tidal frequencies that are present at the surface above the canyon will be observed deeper as internal waves in the canyon.

The canyon morphology has a significant impact on the direction and strength of bottom currents. They are directly controlled by the capacity of the canyon morphology to focus the tidal energy in the canyon axis (Gardner, 1989). The direction of the bottom current is therefore predominantly along the canyon axis, and much less in the cross-canyon direction (de Madron et al., 1999). This explains why the near-bottom currents in the Pointe-des-Monts canyons are mostly oriented along the canyon axis direction through all seasons of the year.

Most of the variance of the along-canyon velocity component is accounted for the semidiurnal internal tides M2 and S2. This is consistent with the observations of Shepard et al. (1979) who demonstrated that the dominant current components in submarine canyons oscillate roughly at the mean tidal frequencies and have two key properties specific to these canyons: currents are dominated by baroclinic (internal) tides, and currents are intensified horizontally towards the canyon head, a finding that is also observed in this study. According to Petruncio et al. (1998) the barotropic tidal currents are focused within the canyon and produce baroclinic tidal currents with speeds of up to 20 cm/s near the bottom at the Monterey

canyon (California) and similarly, in the Pointe-des-Monts canyons, near-bottom horizontal currents have been observed to be in the range of 20-30 cm/s. These currents are likely driven by the baroclinic tidal forces.

Evidence of dynamic interactions with the seafloor has been discovered through velocity and backscatter measurements taken within the Pointe-des-Monts canyons. With near-bottom currents exhibiting a dominant semidiurnal periodicity, these canyons are expected to be particularly dynamic with currents attributed to internal tides that regularly reach 25-30 cm/s at the canyon floors. This is supported by a study conducted by Shepard et al. (1979) that analyzed near-bottom currents in 27 different canyons and found that canyons with tidal periods are the most energetic. The results obtained regarding the occurrence of internal tidal bores suggest that they are likely produced by the presence of internal tides in the canyon head. These internal tidal bores cause sediment resuspension and are thought to transport suspended fine sediments up the canyon. The velocities associated with internal waves with large amplitudes, such as the internal bores in the canyon, are significant enough to lead to sediment resuspension and maintain sediment concentration in the water column (Stastna and Lamb, 2008). The currents of the internal tides can also cause periodic bedload and suspended load sediment in the up-canyon direction (Li et al., 2019). Therefore, it is probable that the internal tidal bores significantly impact the sea bed sediments in the Pointe-des-Monts canyons.

The sediments in the Pointe-des-Monts canyons consist mainly of fine sand (D_{50} = 110–120 μm, Normandeau et al. (2015)). Tests with sediment transport model Sedtrans05 (Neumeier et al., 2008) showed that transport of sand with D_{50} = 115 μm begin when the current 1 m above bed is 30 cm/s (and for D_{50} = 65 μm at 26 cm/s). This suggests that the internal tidal bores in the Pointe-des-Monts canyon are likely to resuspend at least the fine fraction of the canyon sediment. Measurements of bottom currents and sediment transport at multiple locations along the floor of the Pointe-des-Monts canyons would be needed to establish how far up canyons this type of process extend. The relationship between the occurrence

of the internal tidal bores and the baroclinic tidal timing suggests that internal tidal bores are a manifestation of the internal tide. Indeed there is more than 70% occurrence probability of the bores at a specific phase of the internal tide (1.0 ± 0,5 h after low internal tide). This suggests that the breaking of the internal tide is a controlled process rather than a random one. Further studies are required to investigate the underlying physical mechanisms that control the generation and propagation of internal bores.

In addition to internal tidal bores, turbidity currents are the most important process known to cause sediment transport in submarine canyons (eg. Xu et al. 2004; Khripounoff et al. 2003; Paull et al. 2002; Xu et al. 2010). While wave activity has generally no impact on slope stability at depths below 100 meters (Lee and Edwards, 1986), waves have an indirect impact on the Pointe-des-Monts canyons. Turbidity currents observed within the Pointe-des-Monts canyons during this study period (October 2020 to October 2021) and previous observations were all related to storms. This suggests that storms are the principal triggering mechanism of turbidity currents within the Pointe-des-Monts canyons. This is consistent with previous findings of Normandeau et al. (2020), who suggested that with no sediment supply or accumulation in the head of the canyon that could favor turbidity current activity, large waves are likely to be able to trigger turbidity currents in this kind of submarine canyon by increasing bottom shear stress and trigger transport and resuspension of particles. As the destabilized sediments move downslope into the canyon head, they pick up more sediment and become a turbidity current (Sumner and Paull, 2014).

The steep topography of submarine canyons can also contribute to the formation of turbidity currents and increase their density, thereby self-accelerating (Puig et al., 2004). The Pointe-des-Monts canyons have a 20° steep slope down to 75 m that creates a funnel-like effect, which can increase the velocity of the gravity flow and cause it to become more turbulent. The high velocity at the front of the flow suggests that the flow was concentrated at the bottom of the canyon as usual for turbidity current. The two distinct pulses observed during the event can be explained by the dynamics of turbidity currents. The first pulse have

been caused by the initial collapse of a sediment deposit, which generated a dense layer of sediment that rapidly moved down the canyon. The second pulse was probably caused by the collapse of another sediment deposit, which stability may have been weakened by the first collapse. The height of the suspended sediment cloud suggests that the flow was strong and reached a significant distance above the canyon floor. The lack of mooring tilt during this event suggests that although the turbidity current was strong, it did not generate significant lateral forces higher up on the mooring line. The absence of variation in mooring depth after the event suggests that the flow did not cause significant displacement of the mooring and the stability of the sea bed, observed by the backscatter, indicates that the flow did not result in an important sediment deposition around the mooring.

Throughout this study period, only the strongest storm did generate a turbidity current, and no turbidity currents were initiated during periods of only moderate wind and wave energy. Normandeau et al. (2020) documented that turbidity currents in the Pointe-des-Monts canyons were typically caused by storms with wind speeds that exceeded 60 km/h for a minimum of 7 hours, which conditions occurred in the storm of February that triggered the 2021 turbidity current. This can explain why the storms of January 17, 2021, and March 13, 2021, which had wind up to 74 km/h and 68 km/h but lasted only 5 and 4 hours, respectively, did not trigger a turbidity current. The fact that only one of the three major storms during the 2020-2021 deployment triggered a turbidity current and even during the previous years of monitoring not all the storms have triggered a turbidity current suggests that other conditions besides storms may be necessary to trigger these events. This could include the quantity of sediments available at the head of the canyon, the water level, and the presence of surface currents near the canyon head that could influence the turbidity current. Further research may be necessary to identify these additional conditions and to better understand the dynamics of turbidity currents in submarine canyons.

1.8 Conclusion

Analyses of high-resolution velocity and backscatter profiles collected in the head of the Pointe-des-Monts canyons during October 2020 – October 2021 period provided a comprehensive view of the contemporary sediment transport mechanisms operating along this submarine canyon. Two main sediment transport processes with different flow patterns are identified. The first process is the internal tidal bore, which occurs during periods of moderate current velocities associated with bottom-intensified up-canyon flows, which are generated by the presence of semidiurnal internal tides that dominate the flow field and control this sediment transport processes. This frequent transport process involves the resuspension of fine sediments from deeper canyon regions, which may be advected towards the canyon head with the up-slope propagation of the internal tidal bore. The second process is turbidity current, that, unlike the internal tidal bore, transports large volume of sediment associated with down-canyon gravity flows occurring during periods of storms with winds from the NE, cold air temperatures and high waves. All the turbidity currents recorded from 2015 to 2021 in the Pointe-des-Monts submarine canyons occurred in winter months and appeared to be related to storms and probably other conditions unidentified yet.

CONCLUSION GÉNÉRALE

Les canyons de Pointe-des-Monts se distinguent des autres canyons de l'estuaire maritime, car ils sont fréquemment actifs malgré l'absence de l'apport sédimentaire à leur tête. Étant donné qu'ils sont situés sur une pente raide, des instabilités de pente et des processus hydrodynamiques peuvent remobiliser les sédiments environnants, contribuant ainsi à leur activité (Normandeau et al., 2020).

L'analyse des données des ADCP déployés en 2020-2021 dans le canyon le plus actif a permis de déterminer les conditions océanographiques et les processus de transport des sédiments agissant dans les canyons sous-marins. Deux types de processus ont été identifiés qui contribuent à la remise en suspension des sédiments, empêchant ainsi leur dépôt et leur accumulation le long de l'axe du canyon. Ces processus se passent à deux échelles temporelles différentes. Le premier est les mascarets internes. Ce processus est généré par les marées internes, qui sont une caractéristique hydrodynamique commune des canyons sous-marins à travers le monde (Shepard et al., 1979). Ces marées internes à grande amplitude dans le cas de Pointe-des Monts sont générées localement, par les courants de marée barotropiques qui traversent la bathymétrie du canyon. Ces mascarets internes se produisent régulièrement (536 mascarets/an, soit 76 % des marées) et les mesures de l'ADCP démontrent que la majeure partie de la remise en suspension des sédiments est attribuée à ce processus. Ils sont caractérisés par des forts pulses de courants atteignant 25-30 cm/s, qui remontent les canyons et qui peuvent transporter les sédiments fins vers le haut du canyon. Il est possible que le mécanisme de remise en suspension par les mascarets internes puisse également être actif plus loin le long du canyon.

Le deuxième mécanisme est attribué aux courants de turbidité qui sont rares, un seul a eu lieu durant l'année du déploiement étudié, mais beaucoup plus énergétiques que les mascarets internes. Cet événement était composé de deux pulses de courants vers le bas du canyon atteignant 85 cm/s. Ce courant de turbidité s'est produit lors d'une tempête majeure (vents de

65 km/h, hauteur de vague significative de 4,8 m), comme lors des courants de turbidité qui ont été observés à Pointe-des-Monts dans des études antérieures (Normandeau et al., 2020). Bien que les tempêtes soient souvent associées à ces événements, il y a eu d'autres tempêtes qui ont été plus fortes, mais qui n'ont pas entrainé de courants de turbidité. Il est donc possible que d'autres conditions environnementales ou géologiques soient également nécessaires pour déclencher ces phénomènes.

Les courants de turbidité et les mascarets internes sont des agents importants dans le transport et l'accumulation de sédiments dans les canyons sous-marins de Pointe des Monts. Les courants de turbidité transportent des sédiments de toutes tailles en suspension dans l'eau sur de longues distances vers l'aval, tandis que les mascarets internes peuvent transporter des sédiments fins sur des distances plus courtes vers l'amont. L'étude de ces processus est importante. Le cas des canyons de Pointe-des-Monts offre une bonne opportunité pour étudier les courants de turbidités puisqu'ils y sont relativement fréquents. Malgré cette étude et les études antérieures (Normandeau et al., 2014, 2020) l'identification des mécanismes de déclenchement des courants de turbidité, la récurrence des courants de turbidité, les sources exactes du matériel sédimentaire contenu dans les canyons sous-marins de Pointe-des-Monts restent toujours mal compris. Comprendre la fréquence, la force et le fonctionnement de ces courants peut aider à mitiger leurs dangers et évaluer les risques géologiques associés aux instabilités du fond marin.

RÉFÉRENCES

Azpiroz-Zabala, M., Cartigny, M.J., Talling, P.J., Parsons, D.R., Sumner, E.J., Clare, M.A., Simmons, S.M., Cooper, C., Pope, E.L., 2017. Newly recognized turbidity current structure can explain prolonged flushing of submarine canyons. Science advances 3, e1700200.

Babonneau, N., Delacourt, C., Cancouët, R., Sisavath, E., Bachélery, P., Mazuel, A., Jorry, S.J., Deschamps, A., Ammann, J., Villeneuve, N., 2013. Direct sediment transfer from land to deep-sea: insights into shallow multibeam bathymetry at la Réunion Island. Marine Geology 346, 47–57.

Bonneton, P., Van de Loock, J., Parisot, J., Bonneton, N., Sottolichio, A., Detandt, G., Castelle, B., Marieu, V., Pochon, N., 2011. On the occurrence of tidal bores–the garonne river case. Journal of Coastal Research , 1462–1466.

Bourgault, D., Galbraith, P., Dumont, D., 2017. Chapitre 2 : Hydrographie du golfe du Saint-Laurent, In :Archambault P, Schloss I R, Grant C et Plante S.(Eds.) Les hydrocarbures dans le golfe du Saint-Laurent: enjeux sociaux, économiques et environnementaux. Notre Golfe. pp.69-94.

Boyd, R., Ruming, K., Goodwin, I., Sandstrom, M., Schroder-Adams, C., 2008. Highstand transport of coastal sand to the deep ocean: A case study from Fraser Island, southeast Australia. Geology 36, 15–18.

Chiang, C.S., Yu, H.S., 2022. Controls of submarine canyons connected to shore during the lgm sea-level rise: Examples from Taiwan. Journal of Marine Science and Engineering 10, 494.

Clarke, J.E.H., Marques, C.R.V., Pratomo, D., 2014. Imaging active mass-wasting and sediment flows on a fjord delta, Squamish, British Columbia, In: Krastel, S., et al. Submarine mass movements and their consequences. Springer, pp. 249–260.

Codiga, D.L., 2011. Unified tidal analysis and prediction using the utide matlab functions. GTech. rep., Graduate School of Oceanography, University of Rhode Island.Technical Report 2011-01 .

Conway, K.W., Barrie, J.V., Picard, K., Bornhold, B.D., 2012. Submarine channel evolution: active channels in fjords, British Columbia, canada. Geo-Marine Letters 32, 301–312.

Cummins, P.F., Oey, L.Y., 1997. Simulation of barotropic and baroclinic tides off northern British Columbia. Journal of Physical oceanography 27, 762–781.

Cyr, F., Bourgault, D., Galbraith, P., 2011. Interior versus boundary mixing of a cold intermediate layer. Journal of Geophysical Research: Oceans 116 C12029, doi:10.1029/2011JC007359.

Cyr, F., Bourgault, D., Galbraith, P.S., 2015. Behavior and mixing of a cold intermediate layer near a sloping boundary. Ocean Dynamics 65, 357–374.

Ducassou, E., Migeon, S., Mulder, T., Murat, A., Capotondi, L., Bernasconi, S.M., Mascle, J., 2009. Evolution of the nile deep-sea turbidite system during the late quaternary: influence of climate change on fan sedimentation. Sedimentology 56, 2061–2090.

Galbraith, P.S., 2006. Winter water masses in the Gulf of St. Lawrence. Journal of Geophysical Research: Oceans 111, C06022.

Galbraith, P.S., Kelley, D.E., 1996. Identifying overturns in CTD profiles. Journal of Atmospheric and Oceanic Technology 13, 688–702.

Gardner, W.D., 1989. Periodic resuspension in Baltimore canyon by focusing of internal waves. Journal of Geophysical Research: Oceans 94, 18185–18194.

Gordon, R., Marshall, N., 1976. Submarine canyons: Internal wave traps? Geophysical Research Letters 3, 622–624.

Hill, P.R., Conway, K., Lintern, D.G., Meulé, S., Picard, K., Barrie, J.V., 2008. Sedimentary processes and sediment dispersal in the southern Strait of Georgia, BC, Canada. Marine environmental research 66, S39–S48.

Holloway, P.E., 1987. Internal hydraulic jumps and solitons at a shelf break region on the australian north west shelf. Journal of Geophysical Research: Oceans 92, 5405–5416.

Howell, T.L., Brown, W.S., 1985. Nonlinear internal waves on the California continental shelf. Journal of Geophysical Research: Oceans 90, 7256–7264.

Khripounoff, A., Vangriesheim, A., Babonneau, N., Crassous, P., Dennielou, B., Savoye, B., 2003. Direct observation of intense turbidity current activity in the Zaire submarine valley at 4000 m water depth. Marine geology 194, 151–158.

Koutitonsky, Budgen, 1991. The physical oceanography of the Gulf of St. Lawrence: A review with emphasis on the synoptic variability of the motion. The Gulf of St. Lawrence: small ocean or big estuary? Can. Spec. Publ. Fish. Aquat. Sci. 13, 57-90. .

Lauton, G., Pattiaratchi, C.B., Lentini, C.A., 2021. Observations of breaking internal tides on the Australian north west shelf edge. Frontiers in Marine Science 8, 629372.

Lee, H.J., Edwards, B.D., 1986. Regional method to assess offshore slope stability. Journal of Geotechnical Engineering 112, 489–509.

Li, M., Prescott, R., Robertson, A., 2019. Observation of internal tides and sediment transport processes at the head of Logan canyon on central Scotian slope, Eastern Canada. Journal of Marine Systems 193, 103–125.

de Madron, X.D., Castaing, P., Nyffeler, F., Courp, T., 1999. Slope transport of suspended particulate matter on the aquitanian margin of the Bay of Biscay. Deep Sea Research Part II: Topical Studies in Oceanography 46, 2003–2027.

Martín, J., Palanques, A., Vitorino, J., Oliveira, A., De Stigter, H.C., 2011. Near-bottom particulate matter dynamics in the Nazaré submarine canyon under calm and stormy conditions. Deep Sea Research Part II: Topical Studies in Oceanography 58, 2388–2400.

Masunaga, E., Arthur, R., Fringer, O., 2019. Breaking dynamics and associated mixing by internal waves in the coastal ocean. Encyclopedia of Ocean Sciences, 3rd Edition , p.548–554,LLNL–JRNL–749685.

Masunaga, E., Fringer, O.B., Yamazaki, H., Amakasu, K., 2016. Strong turbulent mixing induced by internal bores interacting with internal tide-driven vertically sheared flow. Geophysical Research Letters 43, 2094–2101.

Mertz, G., Gratton, Y., 1990. Topographic waves and topographically induced motions in the St. Lawrence Estuary, in: (M.I. El-Sabh and N. Silverberg, Eds) Oceanography of a Large-Scale Estuarine System. Springer-Verlag, New York, pp. 94–108.

Mulder, T., Zaragosi, S., Garlan, T., Mavel, J., Cremer, M., Sottolichio, A., Sénéchal, N., Schmidt, S., 2012. Present deep-submarine canyons activity in the Bay of Biscay (NE Atlantic). Marine Geology 295, 113–127.

Neumeier, U., Ferrarin, C., Amos, C.L., Umgiesser, G., Li, M.Z., 2008. Sedtrans05: An improved sediment-transport model for continental shelves and coastal waters with a new algorithm for cohesive sediments. Computers & Geosciences 34, 1223–1242.

Normandeau, A., 2015. Processus gravitaires tardi-quaternaires dans les canyons et chenaux sous-marins du Saint-Laurent (EST du Canada). Thèse de doctorat , Université Laval.

Normandeau, A., Bourgault, D., Neumeier, U., Lajeunesse, P., St-Onge, G., Gostiaux, L., Chavanne, C., 2020. Storm-induced turbidity currents on a sediment-starved shelf: insight from direct monitoring and repeat seabed mapping of upslope migrating bedforms. Sedimentology 67, 1045–1068.

Normandeau, A., Lajeunesse, P., Ghienne, J.f., Dietrich, P., 2022. Detailed seafloor imagery of turbidity current bedforms reveals new insight into fine-scale near-bed processes. Geophysical Research Letters 49, e2021GL097389.

Normandeau, A., Lajeunesse, P., St-Onge, G., 2015. Submarine canyons and channels in the Lower St. Lawrence Estuary (Eastern Canada): Morphology, classification and recent sediment dynamics. Geomorphology 241, 1–18.

Normandeau, A., Lajeunesse, P., St-Onge, G., Bourgault, D., Drouin, S.S.O., Senneville, S., Bélanger, S., 2014. Morphodynamics in sediment-starved inner-shelf submarine canyons (Lower St. Lawrence Estuary, Eastern Canada). Marine Geology 357, 243–255.

Paull, C., Ussler, W., Greene, H., Keaten, R., Mitts, P., Barry, J., 2002. Caught in the act: the 20 december 2001 gravity flow event in Monterey canyon. Geo-Marine Letters 22, 227–232.

Paull, C.K., Talling, P.J., Maier, K.L., Parsons, D., Xu, J., Caress, D.W., Gwiazda, R., Lundsten, E.M., Anderson, K., Barry, J.P., et al., 2018. Powerful turbidity currents driven by dense basal layers. Nature communications 9, 1–9.

Petruncio, E.T., Rosenfeld, L.K., Paduan, J.D., 1998. Observations of the internal tide in Monterey canyon. Journal of Physical Oceanography 28, 1873–1903.

Pineda, J., 1994. Internal tidal bores in the nearshore: Warm-water fronts, seaward gravity currents and the onshore transport of neustonic larvae. Journal of Marine Research 52, 427–458.

Pinet, N., Brake, V., Campbell, C., Duchesne, M., 2011. Seafloor and shallow subsurface of the st. lawrence river estuary. Geoscience Canada 38, 31–40.

Pritchard, M., Weller, R.A., 2005. Observations of internal bores and waves of elevation on the New England inner continental shelf during summer 2001. Journal of Geophysical Research: Oceans 110.

Puig, P., Greenan, B.J., Li, M.Z., Prescott, R.H., Piper, D.J., 2013. Sediment transport processes at the head of Halibut canyon, Eastern Canada margin: An interplay between internal tides and dense shelf-water cascading. Marine Geology 341, 14–28.

Puig, P., Ogston, A.S., Mullenbach, B., Nittrouer, C., Parsons, J., Sternberg, R., 2004. Storm-induced sediment gravity flows at the head of the Eel submarine canyon, northern California margin. Journal of Geophysical Research: Oceans 109, (C3):C03019.

Puig, P., Palanques, A., Martín, J., 2014. Contemporary sediment-transport processes in submarine canyons. Annual review of marine science 6, 53–77.

Putra, Y., Noviani, E., Nurhanisa, M., Azwar, A., et al., 2021. A numerical study of hydro-hydraulic energy on undular tidal bore phenomenon, in: Journal of Physics: Conference Series, IOP Publishing. volume 1816. p. 012067.

Shanmugam, G., 2003. Deep-marine tidal bottom currents and their reworked sands in modern and ancient submarine canyons. Marine and Petroleum Geology 20, 471–491.

Shepard, F.P., Marshall, N.F., McLoughlin, P.A., Sullivan, G.G., 1979. Currents in submarine canyons and other sea valleys , Studies in Geology, 8. AAPG, Tulsa.

Stastna, M., Lamb, K.G., 2008. Sediment resuspension mechanisms associated with internal waves in coastal waters. Journal of Geophysical Research: Oceans 113:C10016.

Sumner, E., Paull, C.K., 2014. Swept away by a turbidity current in Mendocino submarine canyon, California. Geophysical Research Letters 41, 7611–7618.

Therriault, J.C., Lacroix, G., 1976. Nutrients, chlorophyll, and internal tides in the St. Lawrence Estuary. Journal of the Fisheries Board of Canada 33, 2747–2757.

Xu, J., Noble, M., Rosenfeld, L.K., 2004. In-situ measurements of velocity structure within turbidity currents. Geophysical Research Letters 31 ,Art. No. L09311.

Xu, J., Swarzenski, P.W., Noble, M., Li, A.C., 2010. Event-driven sediment flux in Hueneme and Mugu submarine canyons, southern California. Marine Geology 269, 74–88.

Xu, J., Wong, F.L., Kvitek, R., Smith, D.P., Paull, C.K., 2008. Sandwave migration in Monterey submarine canyon, central california. Marine Geology 248, 193–212.